System Health Management for Aerospace
Laser-Induced Breakdown Spectroscopy

Lotte van Noetsele

Internship Report submitted to the International Space University in partial fulfillment of the requirements of the M.Sc. Degree in Space Studies

August 2019

Internship Mentor:	**Dr. Robert Stützer**
Host Institution:	**DLR – German Aerospace Center**
	Institute of Space Propulsion – Lampoldshausen
ISU Academic Advisor:	**Prof. Volker Damann M.D.**

This Page Intentionally Left Blank

Abstract

As part of the mission to make human space-travel safer a novel approach for systems health monitoring of rocket propulsion systems using standoff Laser-Induced Breakdown Spectroscopy (LIBS) to measure for wear debris and possible anomalies inside the rocket-engine exhaust plume has been analyzed.

In various experiments, microplasma was created in atmospheric air, in untainted hydrocarbon flames, and in hydrocarbon flames with propagated lithium, table salt, copper, or metal scrap to measure for and detect traces of the elements under the testing conditions.

Traces of the expected elements were detected and confirmed by comparing the spectral fingerprints of the elements with known emission signatures, subsequent proving feasibility of using LIBS to detect element traces, even in luminous gaseous environments using a non-ablative method.

Acknowledgments

I express my most profound appreciation to all those who provided me the possibility to pursue this internship. A special gratitude I give to my mentor at the DLR Institute for Space Propulsion Dr. Robert Stützer, for his guidance, expert advice, and support, and Dr.-Ing. Dipl.-Math Jörg Riccius, of the same institute whom introduced me to the right people at the right time and made this internship happen.

I thank the DLR Institute for Space Propulsion, its support staff, and M.Sc. Michael Börner in particular for providing the facilities, equipment, and tools to conduct my experiments.

I thank Lumibird Quantel-laser for coming to the rescue with a replacement laser that enabled me to complete phase 1 and 2 of my experimentations successfully.

I thank my fellow student Carlo Girardello of the Luleå University of Technology, for getting me up to speed with his feedback, cooperation, and help.

I thank my sister Myrthe van Noetsele of the School for Aeronautics at Embry-Riddle Aeronautical University, for her valued proofreading and comments on this report.

Table of Contents

List of Tables

List of Figures

Nomenclature

Ar	Argon
°C	Centigrade
CaF_2	Calcium Fluoride
Celestial Body	Natural body outside of the Earth's atmosphere, e.g., the Moon, Sun, or Mars
CH_4	Methane
CO_2	Carbon Dioxide
Cryogenic Liquid	A liquid with a normal boiling point below –90°C
ΔT	Temperature difference
Delta-v	Velocity change
fps	Frames per second
g	Gram
GHe	Gaseous Helium
GN_2	Gaseous Dinitrogen
H	Hydrogen
H2	Dihydrogen
H_2O	Water
Hz	Hertz
kg	Kilogram
kN	Kilonewton
LCH4	Liquid Methane
LOX	Liquid Oxygen
LNG	Liquid Natural Gas
Ma	Mach – The speed of sound
mJ	Millijoule
MMH	Monomethylhydrazine
nm	Nanometer
N	Newton (Si unit of force)
N	Nitrogen
N_20_4	Dinitrogen Tetroxide (NTO)
O	Oxygen
O_2	Common allotrope of oxygen
RP-1	Rocket-Propellant-1l
Sec	Second
UDMH	Unsymmetrical dimethylhydrazine

Abbreviations

API	Application Programming Interface
ASD	Atomic Spectra Database
ASHM	Advanced System Health Management
BC	Before Christ
BE-4	Blue Engine 4
BMBF	Bundesministerium für Bildung und Forschung (Federal Institute for Education and Research)
CCD	Charge-Coupled Device
CD	Compact Disc
CMOS	Complementary Metal-Oxide Semiconductor
CTR	Carinthian Tech Research
DLR	Deutsches Zentrum für Luft- und Raumfahrt (German Aerospace Center)
DVD	Digital Optical Disc
EMR	Electro-Magnetic Radiation
ESA	European Space Agency
GPU	Graphical Processing Unit
GTO	Geostationary Transfer Orbit
HiPoLas	High-Power-Laser
ICCD	Intensified Charge-Coupled Device
ISU	International Space University
LEO	Low Earth Orbit
LIBS	Laser-Induced Breakdown Spectroscopy
LUMEN	Liquid Upper stage deMonstrator ENgine
MEMS	Micro-Electro-Mechanical Systems
MSS	Master in Space Studies
NASA	National Aeronautics and Space Administration
Nd:YAG	Neodymium-doped Yttrium Aluminum Garnet (Laser crystal)
NIR	Near Infra-Red
NIST	National Institute of Standards and Technology
NNE	North North-East
PML	Physical Measurement Laboratory
PZT	Piezoelectric
R&D	Research and Development
sCOMS	scientific Complementary Metal-Oxide Semiconductor
SDK	Software Development Kit
SHM	System Health Management

TRL	Technical Readiness Level
UAS	Unmanned Aerospace Systems
ULPM	Upper Liquid Propulsion Module
USB	Universal Serial Bus
UV	Ultra-Violet

1. Introduction

Advanced System Health Management (ASHM) collects and processes system health information throughout every lifecycle, system-wide and for any component using advanced smart sensors, signal processing, data mining, hybrid models (physics and statistics), and failure and life prediction models. ASHM enables sophisticated diagnostics and prognostics to identify system state, detect anomalies, determine anomaly causes, predict future anomalies, as well as system impacts, recommend appropriate mitigation steps, and advances continuously by incorporating new knowledge (Figueroa, et al., 2009).

Propulsion technologies play a crucial enabling role in space transportation and are subject to advanced system health management. Laser-Induced Breakdown Spectroscopy (LIBS) is a technology that potentially can be used to analyze rocket plumes to determine the elements exhausted by the propulsion system. Identifying the elements in the rocket's exhaust can be very helpful to detect wear debris and provides insights in the deterioration process of the engine, making it an intelligible source for system health information that can be used to predict remaining useful life of the rocket engine or specific components and detect problems before they occur. A study to determine the viability of LIBS for system health management applications concentrating on rocket propulsion systems is in the scope of this document.

This internship report is divided into six chapters and describes the performed intern-driven feasibility study to explore the applicability of LIBS in the context of system health management as effectuated at the DLR Institute of Space Propulsion during a 12-week summer internship.

The background of the project, the host organization, and the host's research and development facilities at the Institute for Space Propulsion in Lampoldshausen Germany are depicted in the first chapter.

In the second chapter the theory of space propulsion, system health management, spectroscopy, and laser-induced breakdown spectroscopy, are explained, providing the necessary theoretical information to understand the goals, experiments, and outcomes of the feasibility study.

In chapter three, the equipment, data capturing, data conversion, analytical software, methodology, and the procedures applied during the various experiments are clarified.

Chapter four presents the findings from the experiments and elaborates on the results discovered during the experiments.

Chapter five provides the internship reflection, and the consecutive chapter, chapter six summarizes the conclusions and noteworthy aspects and concludes with an outlook promoting a way forward for future experimentation, research, and development.

2. Background

"I became a pilot; I wanted to fly planes; that was my dream. I never knew though that my mission would become saving human lives. Studying Aeronautical Science at the Florida Institute of Technology college confronted me with the hazards in aviation and aerospace.

The disappearance of Malaysian Airlines flight 370 in March 2014 and the incapacity of the international community to trace the location of the aircraft and its passengers, and the absence of evidence-based conclusions and recommendations, shocked me and made me have a closer look at other tragedies in aviation and aerospace.

I studied the Apollo explosion, the Challenger disaster, and the Columbia Space Shuttle catastrophe that killed the entire crew upon reentry, all because of a piece of broken foam. The problem? The problem was that none of them knew they had a problem until it was too late. 17-deaths because of the inability to communicate potential issues.

I set out to find a solution that would allow for in-the-moment diagnostic hygiene across all mission systems. At that time, I got a movie recommendation from Amazon Video, which uses "artificial intelligence," and then it dawned on me: why not use the power of predictive analytics to make aerospace safer?

That is how Spacevisor was born. Spacevisor is my start-up company's self-learning AI-powered, system-health-management platform that provides predictive analytics that go beyond just reporting statistics and breakages. With this capability, spacecraft can now communicate, across all mission platforms, in real-time, and most importantly, predict future outcomes, autonomously. This means we can now triage these incidents before they play out to a tragic conclusion" (van Noetsele, 2018)

This internship is a significant step in my mission to make space-traveling safer. The concepts of artificial intelligence, predictive analytics, and advanced system health management and their advantages are too abstract for many influential stakeholders in the aerospace industry. A live UAS fleet operations demonstration that uses these advanced techniques and examples of applications in other industries do not connect the dots well enough to let them translate the opportunities of these innovations to their niche in the industry.

Undoubtedly, it takes time to grasp new concepts and ideas. Increasing exposure to these novelties, especially in situations the audience can relate to, will support developing awareness and might even lead to new ideas and discussions on how to apply these innovative concepts. So, why not turn need into a virtue and elaborate on a tangible space-traveling related use case as part of my internship assignment?

2.1 Project

In the search for a compelling showcase for demonstrating the concepts of AI-powered system health management to lecture the target audience and creating value for my mission, I bumped into a technology that has the potential of making space-traveling safer. This enabling technology, which is in itself innovative and hard to comprehend, could enable sensing the elements within a rocket engine exhaust plume from a relatively large and safe distance. Determining the elements in the rocket's exhaust using quantitative and qualitative methodologies, could indicate the wear and tear state of the rocket engine and detect possible anomalies, hence all very valuable information for system health management purposes, especially in combination with predictive big data analytics capabilities.

My initial idea was to bring together a company located in Florida that develops reusable rocket engines, with a Dutch company, specialized in the remote detection technology for other market segments, and my company that would process all the collected data, draw conclusions, make predictions, and show the concept to the world.

A trip with the International Space University (ISU) Master of Space Studies (MSS) Class of 2019 to the Institute of Space Propulsion the German Aerospace Center accelerated the development of my project. Networking during the workshop and linking the activities of the Institute of Space Propulsion with my project idea led to intensive discussions involving the optical specialists of Rocket Propulsion Department, the Dutch supplier of detection technology, and myself on how we could work together to determine the feasibility of the technology for this application.

The fact that my research idea was a new area of research and an exciting topic for the Institute of Space Propulsion made our discussions leading to this 12-week internship to perform a feasibility study and an option to continue afterward as a research assistant.

Thanks to my background in aeronautics, I have ample hands-on experience with applied physics, but I need to expand my proficiency in theoretical and experimental physics, in the field of atomic, molecular, and optical physics in particular, to analyze and dissect the processes involved efficiently.

2.2 German Aerospace Center

The German Aerospace Center DLR (Deutsches Zentrum für Luft- und Raumfahrt, in German) is the federal aerospace research association and includes the space agency of Germany, being in charge of executing Germany's space program. Besides space and aeronautics, DLR also conducts fundamental and product R&D in the field of energy, transport, digitalization, and security to support its mission that focuses on protecting the environment and Earth and Solar System exploration.

DLR's headquarter is in Cologne, and next to its 20 locations throughout Germany, they have offices in Brussels, Paris, Tokyo, and Washington DC. Approximately 8,200 people are currently (2019) employed by DLR. Germany's space budget for 2017 was € 1.5 billion, of which € 860 million was contributed to the European Space Agency (ESA). DLR is also running the largest German project management office, supporting many federal departments and agencies from an organizational and technical perspective. The total budget of DLR in 2017 was €3.8 billion (DLR, 2019).

2.3 Helmholtz Association

DLR is a member of the Helmholtz Association of German Research Centers (Helmholtz-Gemeinschaft Deutscher Forschungszentren, in German). The Helmholtz Association was founded in 1995 and is the largest scientific organization in Germany encompassing 19 autonomous member institutions. Funding provided by the Ministry of Education and Research of the German federal government (BMBF) is distributed via the Helmholtz Association to these globally acclaimed institutions to support the strategic programs in six fields of study: Aeronautics, Earth & Environment, Energy, Health, Key Technologies, Matter, and Space & Transport (Helmholtz, 2019a).

The Helmholtz Association has an annual budget of € 4.7 billion of which ~70% is provided by German federal (90%) and state (10%) administrations. The other ~30% should be attained by the institutions providing contractual research for the private and public sector (Helmholtz, 2019b). Institutions are not funded directly but via competing cross-center research programs using a two-step process focusing on scientific quality.

2.4 DLR Institute of Space Propulsion

The DLR Institute of Space Propulsion (DLR Institut für Raumfahrtantriebe, in German) is located 80-kilometers NNE of Stuttgart near the town of Lampoldshausen in the south-west German state of Baden-Württemberg and is Europe's main rocket-engine test facility. The institute of space propulsion plays a crucial role in safeguarding Europe's independent access to space and develops core competencies in liquid and chemical propellant rocket engines, aiming for reusable rocket engines with higher-thrust while reducing cost (DLR Institute of Space Propulsion, 2018).

A wide range of different test benches are available that can provide the necessary characteristics of the different stages during launch and space flight, enabling developing, testing, verification, validation, and qualification of rocket propulsion systems using cryotechnology and under vacuum conditions.

The ground test program encompasses, amongst others, high-altitude testing for the new ESA Ariane 6 Upper Liquid Propulsion Module (ULPM) for which a new upper stage test bench P5.2 is erected. High altitude testing on earth requires an enclosed inerted vacuum chamber to emulate the operation conditions in space and Earth's upper atmosphere. Test Bench P4 and P5 also allow for space conditions-based testing. Research results from the Institute of Space Propulsion range from Technical Readiness Level 1 (TRL1) to TRL 9 and is the only test site in the world that is involved on all levels, from basic principles design through flight proven products. (DLR Institute of Space Propulsion, 2017).

The DLR Institute for Space Propulsion employs 320 people and is organized into five departments:

- Engineering
- Rocket Propulsion,
- Propellants
- Safety, Quality, and Facility Management
- Test Facilities

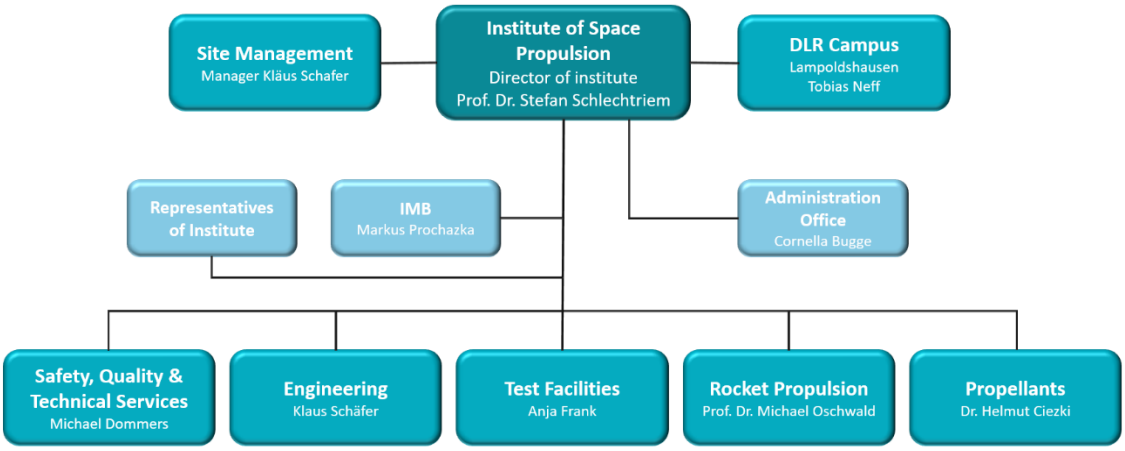

Figure 2.1. Organizational Structure of the DLR Institute of Space Propulsion (DLR Institute of Space Propulsion, 2017)

Engineering

The Engineering Department is responsible for the development and design of launchers and propulsion system test facilities. Some strategic proficiencies include engine control

systems, data collection, data analytics, monitoring, command and control systems, and altitude simulation.

Rocket Propulsion

The Rocket Propulsion Department conducts fundamental research of propulsion systems inner workings and develops propulsion application technologies, concentrating on end-to-end propulsion solutions. As part and under the guidance of the rocket propulsion department team, with support of other departments, the feasibility study as described in this report was conducted.

Propellants

The Propellants Department conducts R&D activities to investigate the applicability of potential propellants for spacecraft and launch systems, using physicochemical analysis methodologies to determine the nature of interactions between components based on the physical properties and composition in conveyors, tanks, and thrust chambers.

Safety, Quality, and Facility Management

The Safety, Quality, and Facility Management Department is responsible for the safety of people, facilities, and the environment. The department provides site security, site safety, medical assistance, operates the safety and emergency management system, a fire station, a water treatment plant and other onsite utilities, and maintains the facilities integrated management system.

Test Facilities

The test facilities department plans, builds, and operates the test facilities for propulsion systems and works closely together with the European space industry, especially with the ArianeGroup, whom also have offices on-site and run tests in cooperation with DLR on behalf of ESA.

There are two different types of test bench facilities at the DLR Institute for Space Propulsion, sea-level test, and altitude simulation test benches. Other onsite facilities include laboratories like the Physicochemical laboratory and supply systems that provide the necessary supplies needed for testing like the Liquid Hydrogen fuel storage, Liquid Oxygen fuel storage, cooling water supply, wastewater treatment, and production plants for GN2 and GHe (DLR, n.d.a).

The current allocation of the test benches is as follows (DLR, n.d.c):

Test Bench P1

Altitude condition simulation for small propulsion systems (<=600 N) using mono-methyl hydrazine (MMH) and dinitrogen tetroxide (N2O4) propellants.

Test Bench P2

Ground test facility operated by the ArianeGroup for testing under sea-level conditions limited to approximately 30 kN.

Test Bench P3

Testing facility for a new propellant combination of LOX and CH4.

Test Bench P4.1

Vinci upper stage rocket engine testing with and without high altitude simulation.

Test Bench P4.2

Eastus upper stage rocket engine testing with and without high altitude simulation.

Test Bench P5.1

Vulcain 2 cryogenic first stage main rocket engine testing at sea-level.

Test Bench P5.2

Complete cryogenic testing of the Ariane 6 upper stage ULPM with high altitude simulation.

Test Bench P6.1

Cryogenic high-pressure combustion testing.

Test Bench P6.2

Nozzle flows and high-altitude simulation.

Test Bench P8

Research for next-generation high-pressure rocket propulsion systems.

Test Bench Complex M11

Multiple test positions, each with a set of different test conditions for combustion testing with a broad spectrum of rocket propellants (DLR Institute of Space Propulsion, 2016).

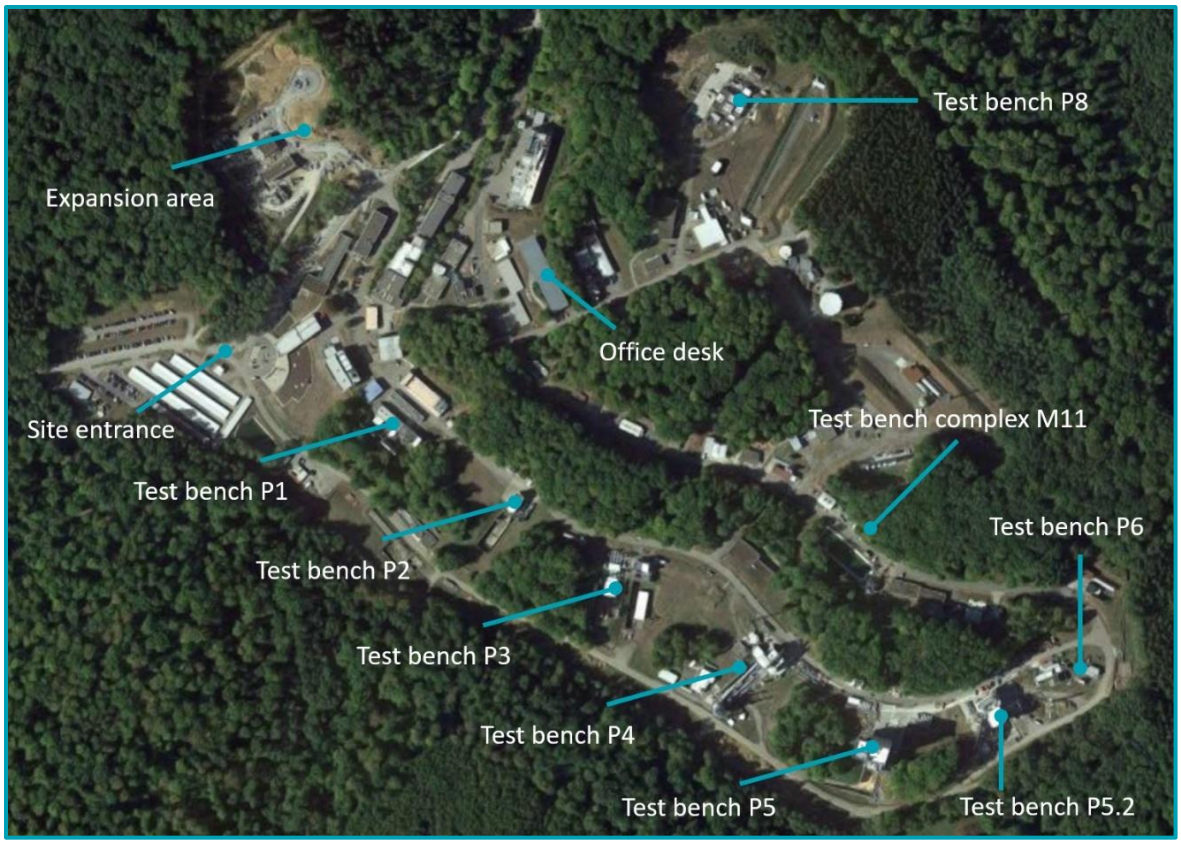

Figure 2.2. Satellite photo of the DLR Institute for Space Propulsion (Google Maps, 2019)

3. Theory

3.1 Rocket Systems

The working principle of a rocket is based on Newton's 3rd law of motion. Action and an opposite reaction come as a pair, the velocity of the exhaust plume creates an equal opposite reaction, providing thrust to the rocket. The actual acceleration depends on external factors like gravity. The escape velocity from Earth's gravity is ~11.186 KM/s. The speed of moving to destinations within the earth-moon system is lower than the escape velocity. To move from the earth's surface to LEO, at least 9.4KM/s delta-v is needed, plus additional speed to compensate for atmospheric drag. Movements not subject to the gravity of celestial bodies require much lower delta-v (Swinerd, 2008).

The purpose of a rocket for spaceborne activities is to transport a payload to earth's orbit or beyond. The total weight of the fuel and the rocket components consume a huge part of the total possible mass, leaving very little to no space for the actual payload. To allow for more payload capacity, a rocket launched from the earth is made of multiple stages to reduce its mass by dropping dispensable parts during flight, like empty fuel tanks,

rocket boosters, and the main engine of the first stage. For example, the ESA Ariane 5 ECA rocket has a liftoff mass of 780,000 KG and a net payload mass of 10,000 KG to GTO and 21,000 KG to LEO, a payload fraction of 1,28% and 2.69% respectively (ESA, 2016).

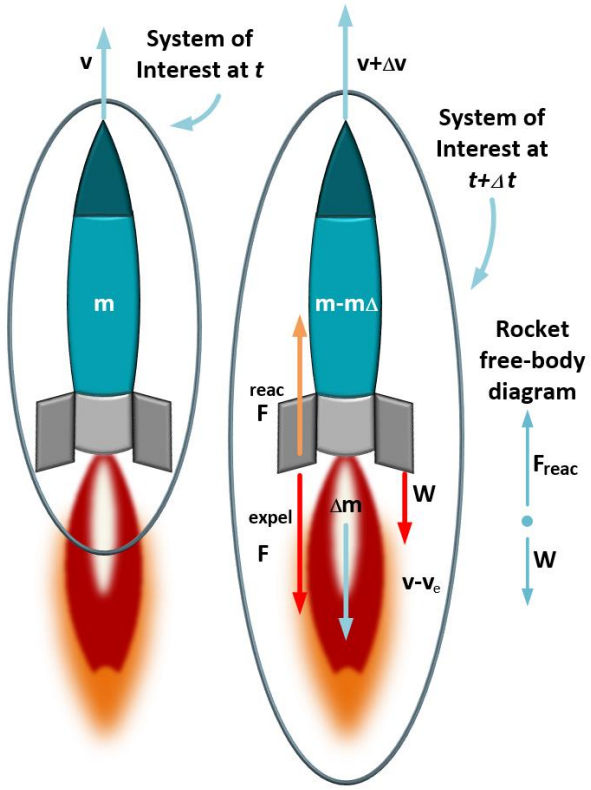

Rocket propulsion diagram:

(a) The rocket depicted on the left has a mass m and an upward velocity v. −mg is the net external force on the system if neglecting atmospheric drag;

(b) At time Δt later the rocket system as depicted on the left has two principal parts, the gas ejected from the rocket and the rocket itself. The gravitational force is overpowered by the reaction force on the rocket and accelerates it upward (Embry-Riddle, 2019).

Figure 3.1. Rocket propulsion diagram (Embry-Riddle, 2019)

3.2 Chemical Rocket Propulsion Systems

A rocket engine differs from a jet engine as used on aircraft in that they do not use air from the atmosphere as the oxygen source. A rocket can operate independently from its environment, since all working fluids to propel the rocket, including oxygen, are stored onboard the rocket, allowing it to work under atmospheric and vacuum conditions.

The most common type of rocket engines are chemical combustion engines that use a mixture of fuel and oxidizer as the propellant. These chemical rockets use liquid, solid, or hybrid propellants that are highly pressurized and generate an exothermic reaction in the combustion chamber, producing hot gases that expand in the nozzle and are accelerated by the supersonic shape of the nozzle to even higher velocities, providing trust to the rocket. All rocket parts that are exposed to these hot gases that can vary in temperature from 2,500 to 4,000 °C need to be insulated or cooled. A popular design is to cool the combustion chamber and the nozzle by circulating the cryogenic liquid propellants in small tubes around them. The pressure needed to pump the propellants into the

combustion chamber must be higher than the already very high pressure in the combustion chamber.

There are two distinct types of liquid rocket propulsion, Boost Propulsion to propel the vehicle along its trajectory, and Auxiliary Propulsion for trajectory correction, small maneuvers, altitude alterations, and upkeeping orbit. The booster stage is applied in the main and higher stages of launch vehicles and needs a few seconds to reach full trust; auxiliary propulsion can be found in satellites and spacecraft and reaches full trust very fast (0.004–0.080 sec). Another significant difference between the two propulsion types is the liquid propellant used. Where boost propulsion relies on cryogenic and storable liquids, auxiliary propulsion depends on storable liquids, monopropellants, or stored cold gas. Auxiliary propulsion is often not liquid-based, for smaller corrections and orbit maintenance ion thrusters that use Xeon or Krypton as propellant are increasing market share (Biblarz and Sutton, 2016).

3.3 Propellant

Prevalent liquid propellant types for booster propulsion are Liquid Oxygen with Kerosene (LOX/RP1) and Liquid Oxygen with Hydrogen (LOX/H2). Liquid Oxygen with Liquid Methane (LOX/MH4) is currently under development at many launch vehicle operators, e.g., Blue Origin's BE-4 engines, SpaceX' Raptor engines, and ESA/DLR's LUMEN project. Methane is performing better than the best storable liquid propellants. Methane is also more stable and requires less cooling than Hydrogen (-162 °C instead of -253 °C), has a higher density, requiring less mass for the storage tank than Hydrogen rockets, but is harder to ignite than Hydrogen (Biblarz and Sutton, 2016).

Burning methane is a straightforward exothermic combustion reaction that releases carbon dioxide, water, and (lots of) energy only; making it the cleanest fossil fuel. Liquid Natural Gas (LNG) is a hydrocarbon gas that mainly exists of methane and releases fewer waste products compared to other fossil-based fuels.

Hydrazine and UDMH are two other propellants that can use LOX as an oxidizer. Fluorine can be used as an oxidizer with Hydrazine and Hydrogen, and Nitrogen Tetroxide with Hydrazine, a 50/50 mix of Hydrazine and UDMH, RP1, and Monomethylhydrazine (MMH).

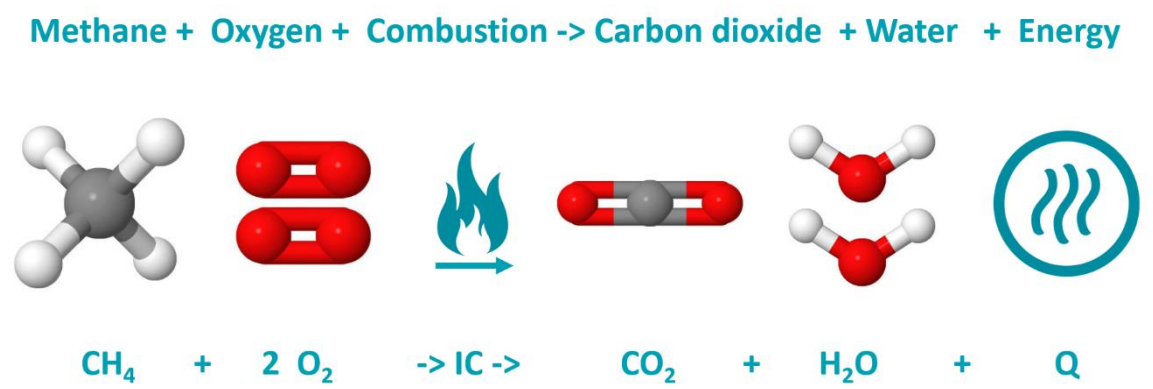

Figure 3.2. The properties of Methane make it a promising propellant

3.4 Nozzle

The rocket engine nozzle is shaped to converge the thermal energy released in the combustion chamber down the throat of the nozzle, accelerating the hot exhaust gases ideally to a speed of Mach 1. In the divergent section of the rocket, the flow is expanded downstream to a propulsive force with supersonic Mach velocity towards the end of the nozzle. The optimum expansion equals a local ambient pressure at the nozzle's exit; this means that an optimum expansion is not possible during the complete trajectory from sea-level to space with a static nozzle.

Much of the thermal energy converts into kinetic energy in a converging-diverging nozzle. The inside of the nozzle must be smooth without irregularities, as the kinetic energy can reverse into thermal energy where the flow in the nozzle is obstructed by irregularities on the surface, overheating and quick deteriorating the nozzle (Biblarz and Sutton, 2016).

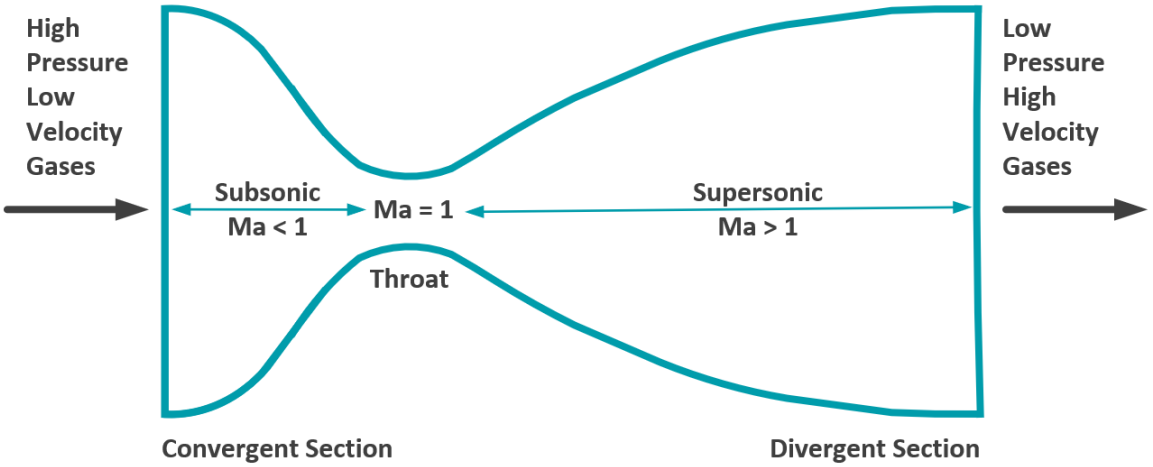

Figure 3.4. Rocket engine nozzle

3.5 System Health Management

System Health Management (SHM) is a branch of system engineering and expands on traditional safety and reliability engineering from functional design, system design, system development, system operation, to complete system life cycle with the goal to reduce risk by assuring safe and undisrupted operations, even under off-nominal conditions like those in hazardous and extreme environments. A crucial observation in SHM is that system failure might not be preventable; they are often predictable, given the proper hybrid physics and statistic-based models using advanced smart sensors, signal processing, and data mining techniques.

SHM focuses on providing capabilities to identify system state, detect anomalies, diagnose anomaly causes, avoid or respond to and recover from anomalies, predict future anomalies and system impacts, and provide timely prevention or mitigation of anomalies, to assure continuous nominal system operations.

A relatively small quantity of system failures originates from environmental causes or projected wear outs of system components. Human errors, on the other hand, are the major factor for most system failures. Misperceptions, miscommunication, and the lack of communication cause design flaws, engineering faults, and human operational errors. Design flaws are repeated in all duplicates of a system, whereas an engineering fault usually occurs in only one copy of the system, and operational errors are one-time mistakes by operators. If engineering faults and human operational errors arise more than once over the identical duplicates, a design flaw in the system or the ergonomics design is usually the cause. Reducing system failures introduced into the system by human error is one of the most critical domains in System Health Management (Johnson, et al., 2011).

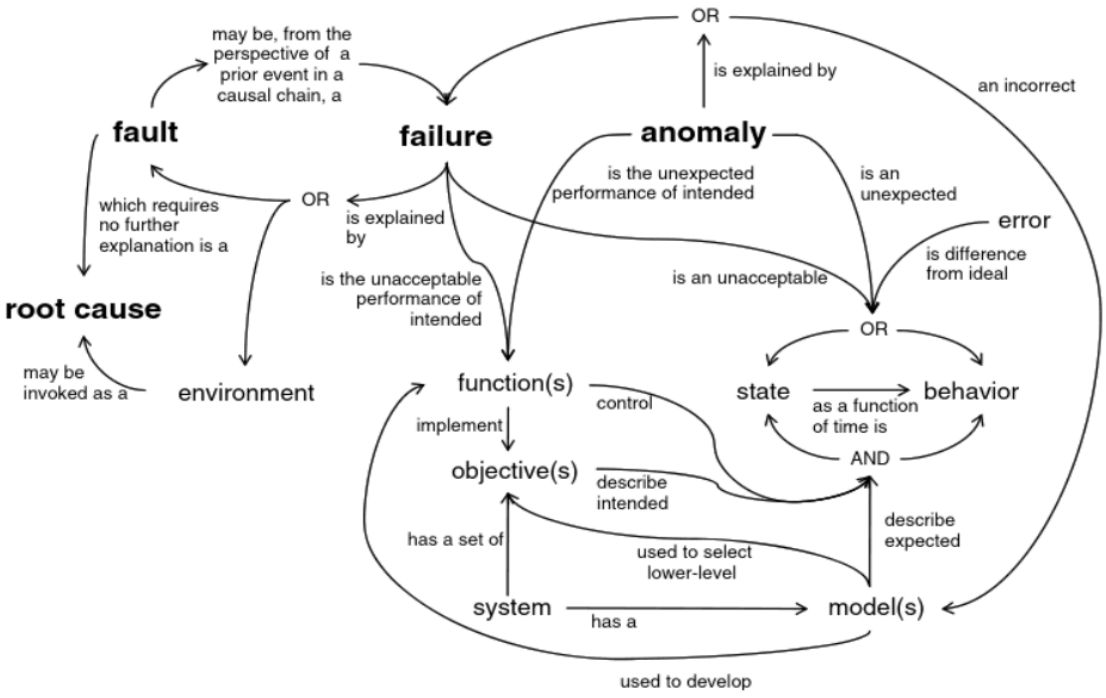

Figure 3.5. Concept diagram of major SHM terms (Johnson, et al., 2011)

Preventing, analyzing, and mitigating failures to make systems more dependable is the core purpose of SHM. Strategies to safeguard the function of the system are:

- avoiding faults during designing
- avoiding faults during manufacturing
- avoiding faults during operations
- mask failures
- failure recovery
- change goals

System Health Management should be an integral part of the end-to-end design and not a later add-on. For both structural health management and engine health management data to determine the health status can be collected using, for instance, remote, wired, and wireless smart sensors, nondestructive testing/evaluation, high temperature and fluid leak detection, thermoelastic stress analysis, digital image correlation, IUT bearing condition monitoring, advanced mechanics, and fusion of sensor data. Typical sensor types are capacitance, strain gauges, crack sensors, piezoelectric PZT, thin-film thermocouple, ultrasound, Micro-Electro-Mechanical Systems MEMS, fiber brag grating, carbon nanotubes, thermography, eddy current, spectroscopy, and more.

3.6 SHM Rocket Propulsion Systems

Propulsion systems are core enablers of every space mission, from deploying satellites in low earth orbit to deep space exploration missions. To realize successful missions, the safe and dependent operations of propulsion systems is a critical aspect (Garg, Maul and Melcher, 2007).

The increasing practice of reusing launch propulsion systems requires even more precise system health information. Real-time acquisition of health data enable decision-making during the launch whether the fuel is used to land the booster or rocket stage in a controlled way so it can be recovered and inspected for possible reuse, or to use the fuel to attain extra height ensuring the rocket stage and propulsion system burn up in the atmosphere.

A detected deformation of the nozzle, large amounts of wearing debris in the rocket plume, leaks in the tanks, or anomalies in the combustion are all valid reasons not to consider the reuse of the rocket stage and the propulsion system. An anomaly could also be a reason to recuperate and analyze the propulsion system.

Figure 3.6. System Health Management for propulsion systems impression (Alamgir, 2019)

3.7 Plasma

Matter exists in the four classical states, solid, liquid, gas, and plasma. Changes in pressure or temperature can induce the transition from one state into another. There are many known intermediate and exotic states that exist under specific or extreme environmental

circumstances only. Plasma is the most abundant known state of matter in the universe, mainly because stars are big bodies of plasma. (Gurnett and Bhattacharjee, 2005) estimate that 99% of the visible universe consists of plasma. On Earth plasma is rare in contrast to solids, liquids, and gasses. A part of the Earth's upper atmosphere, the ionosphere consists of plasma ionized by electromagnetic radiation from the sun.

Melting and freezing are state transitions between solid and liquid, vaporizing and condensation between liquid and gas, and ionization and deionization are the state transitions between gas and plasma. Ionization breaks free electrons and changes gas into plasma, like other state transitions under the influence of pressure and temperature. The plasma contains free electrons and positively charged ions.

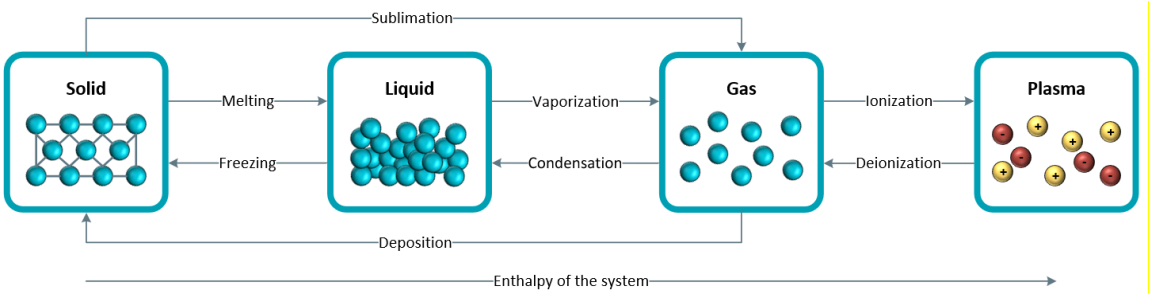

Figure 3.7. Phase transitions between the classical states of matter (UC Davis, 2019)

Natural plasma occurs in all types of lightning, the ionosphere, and the polar aurorae. Under ambient sea-level conditions, plasma rapidly deionizes, unless confined in, for example, an energized tube like a fluorescent neon light (NASA, 2001). Artificially created plasma can be found in plasma displays, fluorescent lamps, arc welders, plasma balls, during re-entry of a spacecraft into the atmosphere in the area in front of a heat shield, and in rocket exhausts (Plasma Universe, n.d.).

The state of plasma is used in ion thrusters for space propulsion. Nevertheless, since these are not subject to the project, we will only focus on chemical propulsion, where thermodynamic values are not sufficient for plasma generation. Hence, we have to induce the state of plasma into or onto our research object. One way to take advantage of an electron-ion-recombination inside a combustor is laser-induced ignition: A focused beam of laser light generates a plasma cloud by ionizing a sufficient number of atoms of the targeted material. In a minuscule timeframe, the plasma expands at supersonic velocities accompanied by an audible clicking sound caused by the expansion shockwave and a visible light flash (More, 2017). However, a plasma can be induced wherever and whenever in the combustion zone for research and health monitoring purposes. The spectral analysis of light, emitted from the laser-induced plasma cloud is called laser-induced breakdown spectroscopy (LIBS).

3.8 Optical Spectroscopy

Energy is carried in electromagnetic radiation (EMR) waves (Photons) of a broad range of wavelengths that are visible only between 400 and 750 nm. A device capable to quantitatively disperse photons by wavelengths is called an optical spectrograph. Therefore, optical spectroscopy delivers intensity values as a function of photon wavelengths. The wavelength regime of interest for our investigations ranges from the ultra-violet (UV) to the near infra-red (NIR) radiation. However, when a photon hits a particle of any matter, a change within the particle occurs. Spectrometry indirectly studies these interactions between light and matter by using the radiation intensity and wavelength measurements mentioned above.

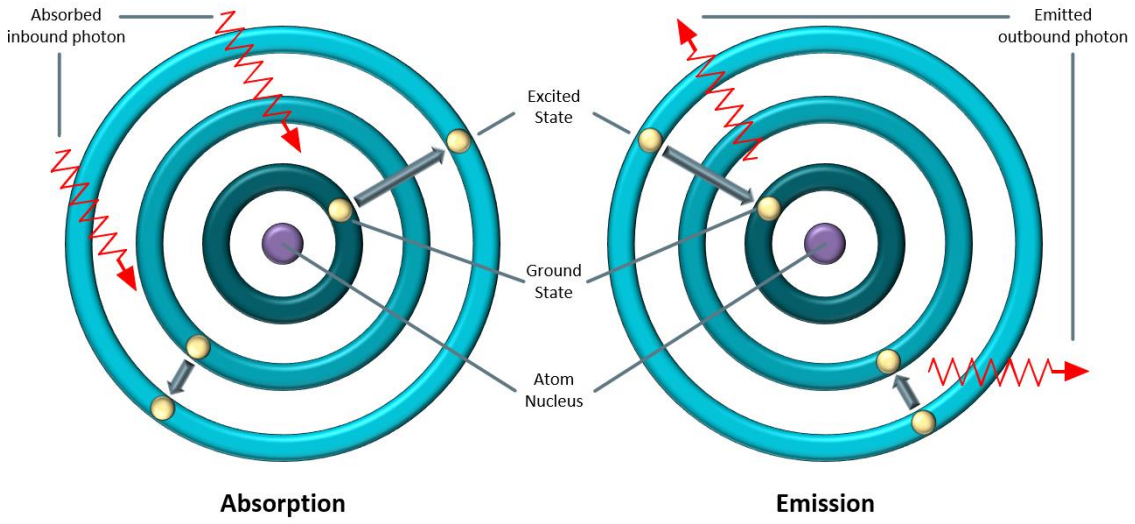

Figure 3.8. The energy characteristics of the emitted photon are identical to the energy of the absorbed photon, allowing identification of the atom by its emission spectrum

Absorption and Emission are two ways of interaction between electromagnetic radiation and matter. Electrons in particles jump from ground-state to excited state when hit by electromagnetic radiation, and one or more photons are absorbed. When electrons in particles fall back from excited-state to ground-state, they release photons; this is called emission. The classical distance between electrons and the atomic nucleus is the smallest possible in the ground state, and the energy level is constant at a minimum level. In the excited state, the energy level is always higher than in the ground state, but the level varies depending on how many electrons are in the excited state at the same time. The excited state is highly unstable and has a very short lifetime (Bernath, 2015., Kenyon, 2011 and Richmond, 2012)

Each atom and molecule in nature absorbs and emits a specific combination of electromagnetic wavelengths, providing a unique absorption and emission spectrum, also called fingerprints, enabling the detection, identification, and quantification of atoms and molecules. For instance, cooling down plasma in a rocket engine's exhaust emits the unique spectral signature of the atoms, and the element of the atoms can be identified using a spectroscope.

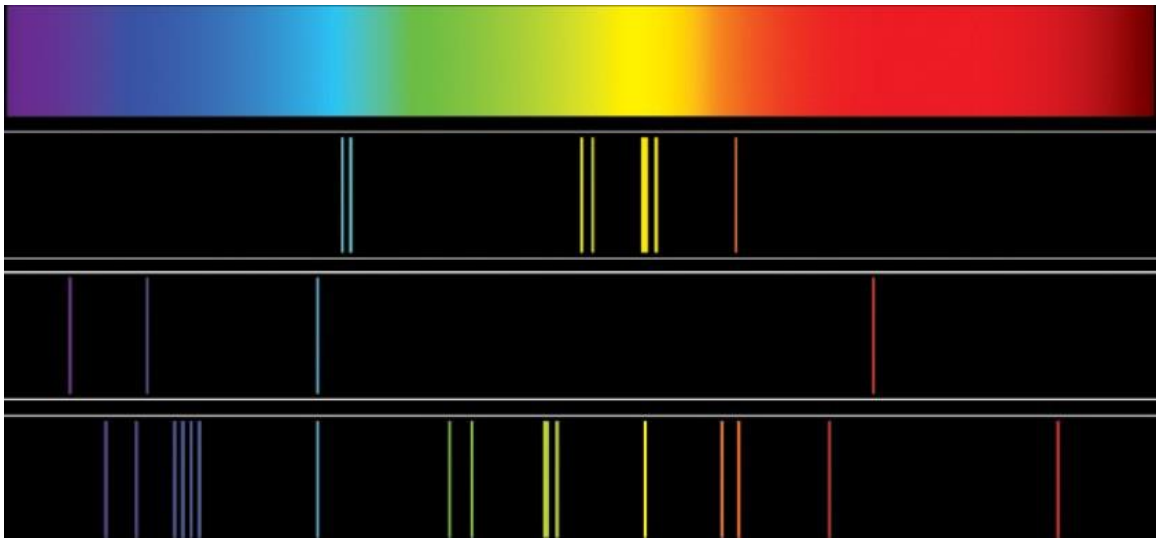

Figure 3.9. The first horizontal bar displays the whole spectrum of "white" light as emitted by the Sun. Bar two, three, and four are the unique optical radiation emission signatures or fingerprints of respectively Sodium, Hydrogen, and Calcium. (Bob, 2018)

3.9 Laser

Laser is the abbreviation of Light Amplification by Stimulated Emission of Radiation. A laser generates a coherent light beam and is used in countless applications and devices. In a Compact Disc (CD) and DVD player, for instance, the laser light scans the disc that contains data in a spiral pattern of pits and lands, and these pits and lands reflect the light with different intensities onto a photodiode that converts the light into an electrical current. A CD is scanned using a 780 nm wavelength laser. To increase the storage capacity of the disc, data needs to be compressed more, by narrowing the width of the spiral and sizes of the pits and lands and space in between, requiring a laser with a shorter wavelength, i.e., for DVD 650 nm, and 405 nm for blue-ray (Peek, 2010). Well-known laser applications are bar code scanners in shops, laser printers, laser pointers, skin and acne treatments, hair and tattoo removal but lasers are also used guiding missiles, fingerprint detection, and for industrial cutting and welding and also in medical surgery. A laser produces and amplifies a powerful beam of light in one direction lined up on the same frequency with a relatively constant phase and maintaining a bright narrow beam of parallel rays of light over great distances.

The essential properties of laser beams are:

- Monochromaticity
- Coherence
- Directionality
- Brightness

Lasers have three key components:

- Pump source
- Gain medium
- Resonator of two mirrors

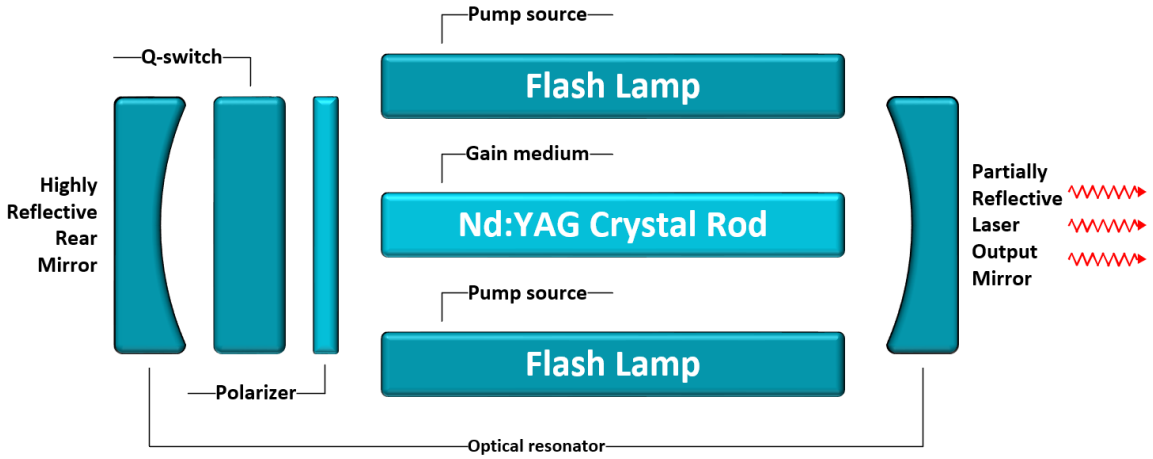

Figure 3.10. Schematic of a flash pumped active Q-switched Nd:YAG laser

The pump source is a source of light, e.g., a flashlamp adding energy to stimulate the medium. The gain medium amplifies emitted electromagnetic radiation by transferring energy into it of a wavelength that depends on the properties of the used medium and therefore determines the color of the laser light since the emitted photons during the stimulated emission are all of the same wavelength. The resonator keeps photons bouncing back and forth between the two mirrors inside the medium supporting population inversion and increasing stimulated emission (Hänsch and Träger, 2007).

There are many types of lasers, gas lasers, chemical lasers, dye lasers, metal vapor lasers, solid-state lasers, and semiconductor lasers, to name a few. The semiconductor laser is used in compact discs players and chemical lasers by the military.

A laser can be used to create plasma on a microscopic scale generating a unique emission signature by the photons emitted by the atom when cooling down that can be captured using spectroscopy. Many types of lasers can be used for this purpose. Solid-state lasers, especially crystal-based Nd:YAG lasers are vehemently used for this purpose, especially those that use Q-switching, a method used to generate very powerful narrow laser pulses.

Diode-pumped Nd: YAG lasers have a small form factor and a great pulse to pulse reproduction but are more expensive than Xe-arc flash lamp pumps (Musazzi and Perini, 2014). Nd:YAG lasers are available with water or air cooling, a wide range of output powers, varying pulse length, repetition rates between 1-100Hz, and the well-known photon wavelength of 1064 nm, which can be phase doubled to 532 nm, phase tripled to 266 nm and so on.

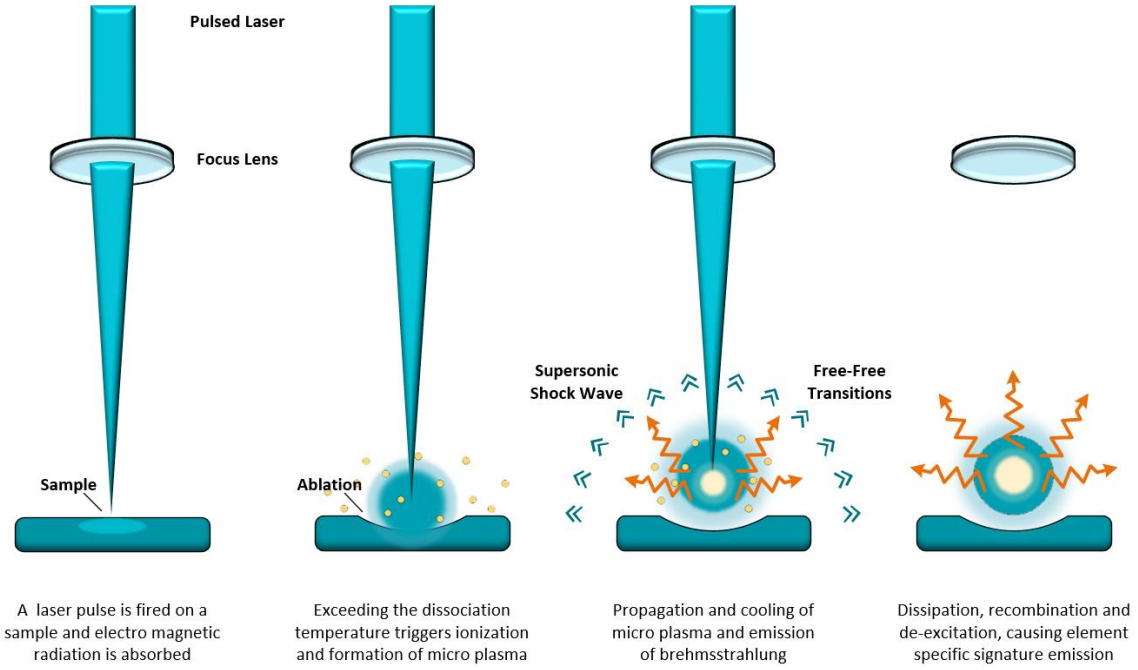

Figure 3.11. Laser-induced plasma forcing signature emission to identify matter

3.10 Laser-Induced Breakdown Spectroscopy

LIBS is a non-invasive, non-destructive elemental analytical spectroscopic technology that can detect, identify, and quantify the elemental composition of solids, liquids, gasses, and aerosols in real-time. LIBS is using a focused pulsed laser beam that ionizes one or more atoms of the targeted matter resulting in an intense atomic emission as the plasma cools down. State-of-the-art spectrographs work with optical intensifiers that convert photons into electrons which are amplified using a high-voltage cascade. Hence, the generated electrons hit a phosphor screen in order to be reconverted into visible photons for spectrometry. Moreover, the intensifier can be used to define optical recording parameters such as gate width, delay time, and gain (Musazzi and Perini, 2014).

LIBS can be applied over relatively long distances with low power lasers and telescopic lenses, facilitating analyses of contaminated and other hazardous environments. The trend in recent years to manufacture ever-smaller mechanical, optical, and electronic devices resulted in compact portable and easy to integrate LIBS devices. For System Health Management, LIBS can be integrated as a smart sensor for monitoring purposes.

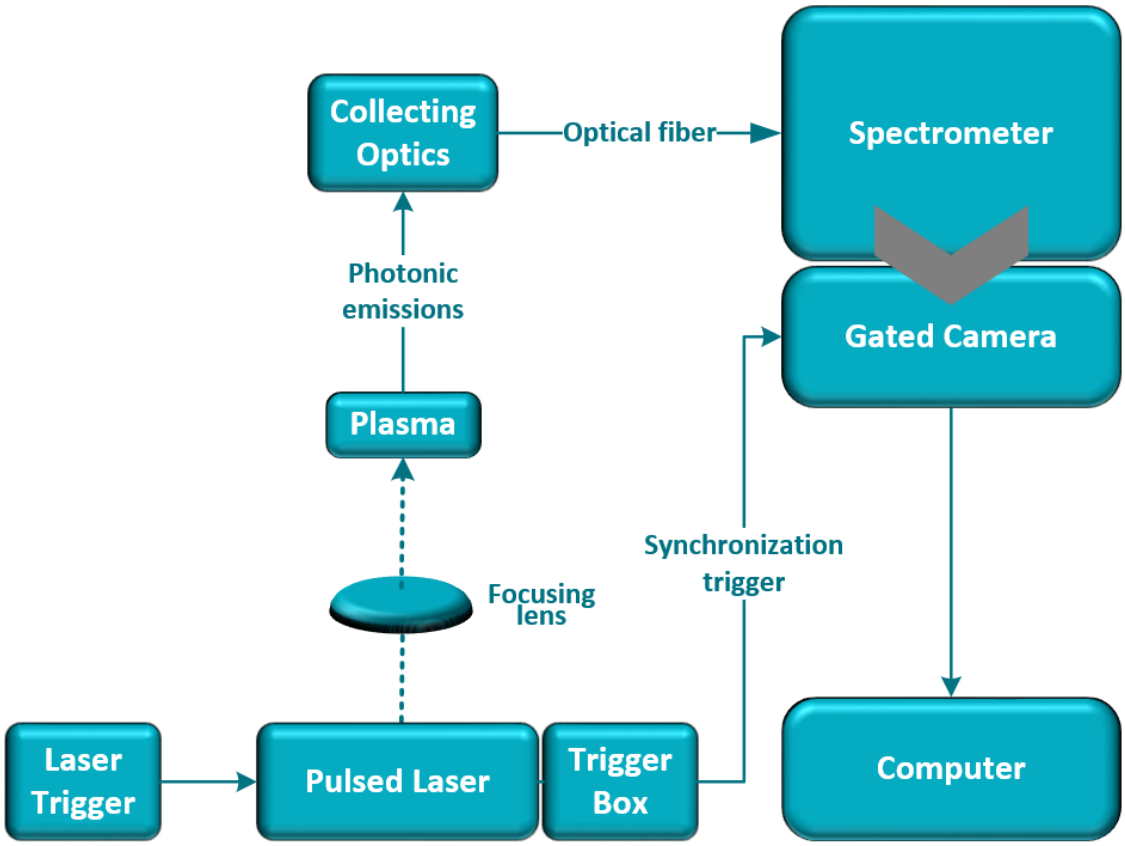

Figure 3.12. Diagram of a typical LIBS setup

4. Experiments

In this section, the used experimentation methodologies and equipment to determine the viability of using (stand-off) Laser-Induced Breakdown Spectroscopy (LIBS) as a means to collect data from the rocket engines exhaust are explained. The composition of the rocket plume is a potential source for qualitative and quantitative data to determine the efficiency of the combustion, wear and tear of the rocket engine, pumps and nozzle, and detect possible other anomalies. The rocket exhaust plume is expected to contain traces of elements from wear debris that can provide insights into the deterioration process of the engine. We expect we cannot measure the efficiency of the used propellant mix since the combustion process releases new molecules, though the elemental composition stays the same, and with LIBS, we can identify elements, not molecules. To be able to detect molecules, we would need technology like Raman spectroscopy.

The miniaturization of LIBS equipment in recent years enables the application of the technology outside a laboratory environment, for instance as a built-in sensor in the nozzle or the combustion chamber of the rocket engine and feeding the data to an

integrated system health management solution that monitors the complete ecosystem and correlates measurement data from all sources.

4.1 Test Facilities

Test bench P8 of the DLR Institute of Space Propulsion site in Lampoldshausen was built as a test facility for high-pressure combustion with hydrogen and liquid oxygen. DLR runs the shared facility with two test cells allowing up to 100 tests a year. Each test cell is utilized with a noise suppression system and two diagnostic rooms that can be used to install measurement equipment. Soon, the facility will provide the option to use a vacuum system to facilitate high altitude tests as well.

Operating the P8 Test Bench is the responsibility of the DLR Test Facilities department, and the primary users are DLR, ArianeGroup, and the French Space Agency CNES. The frontend measurement and control systems are located at the P8 test facility. The central operations control room for P8 is located at building D68 and uses a decentralized real-time computer system. Due to the construction of the new P8.3 test cell, the P8 Test bench is at the moment available for testing on Mondays and Tuesdays only.

Figure 4.1. Test Bench P8 (DLR Institute of Space Propulsion, 2018)

The P8 Test bench is used mostly for fundamental research, like testing new concepts of propulsion, verifying and validating new ignition methods (e.g., laser), injection solutions, new materials (e.g., ceramics), and collecting calibration data for verification and validation (Stützer, Börner and Oschwald, 2018). Moreover, advanced manufacturing techniques and test bench solutions for noise suppression, altitude systems, and

supersonic diffusers are developed using the P8 Test bench facilities (DLR Institute of Space Propulsion, 2017).

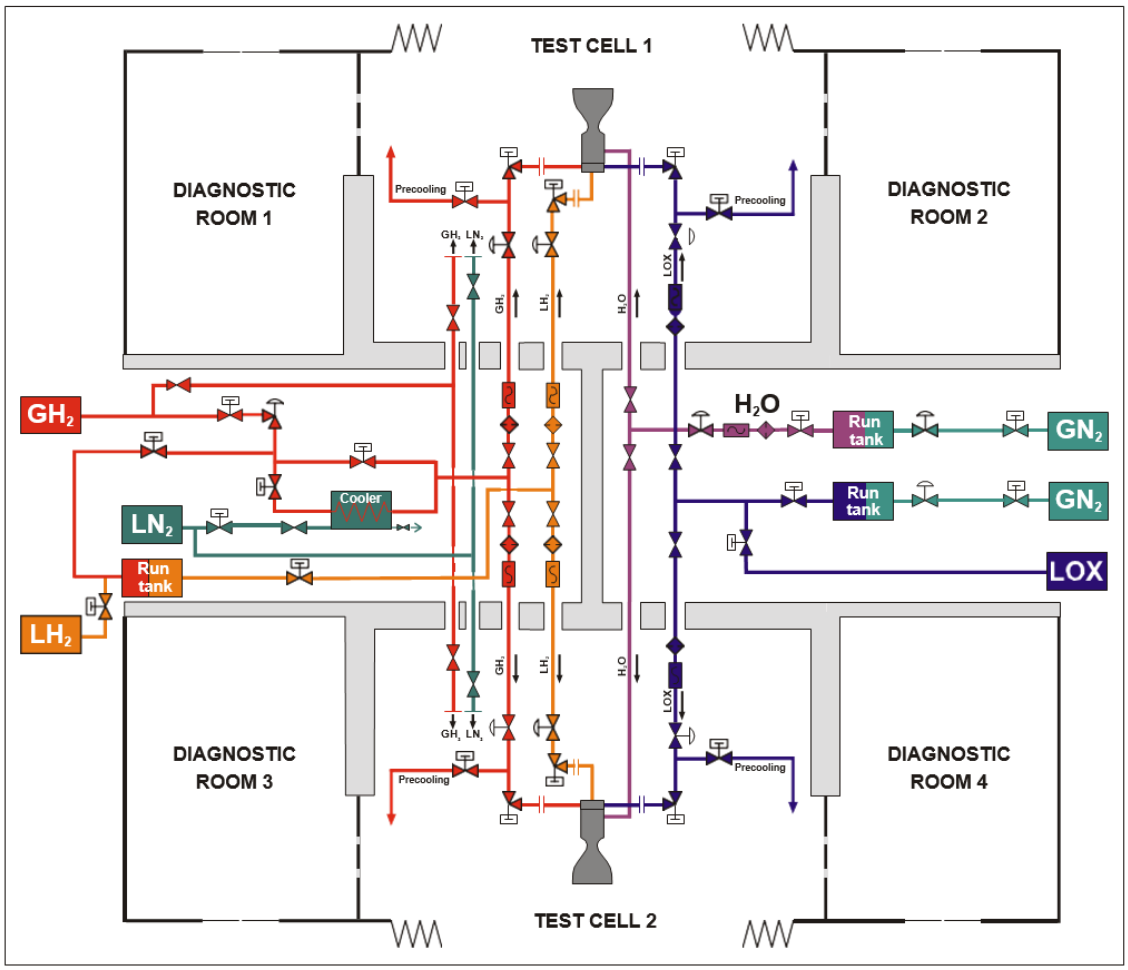

Figure 4.2. Test Bench P8 floor and cryogenic piping plan (DLR Institute of Space Propulsion, 2007)

The LUMEN Program

The LUMEN Program (Liquid Upper stage deMonstrator ENgine) is a DLR R&D program that started in 2014 and currently uses P8.1 (P8 Test bench cell 1) to develop and test complete engine cycles of a pump-operated LOX/LCH4 upper stage rocket propulsion engines of the expander bleed type. The LUMEN engines are small-scaled compared to others but have a high level of thrust. The demonstrator engine's full thrust power of 30 kN is comparable with rocket engines for flight. The LUMEN project also uses a new method to ignite the propellant based on laser ignition technology (DLR Institute of Space Propulsion, 2017 and Deekena, et al., 2017).

Under the LUMEN program, multiple research projects using optics have been conducted, but none of them used LIBS to analyze the rocket plume as anticipated in this research

project. However, a recent research project used LIBS technology to collect data from processes inside the combustion chamber. Since the combustion was ignited using laser-induced plasma breakdown events, the radiation, emitted by the electron-ion-recombination, could be collected by line-of-sight sapphire probes, a fiberglass cable and an optical spectrograph, triggered by the laser beam (Stützer, Börner and Oschwald, 2018).

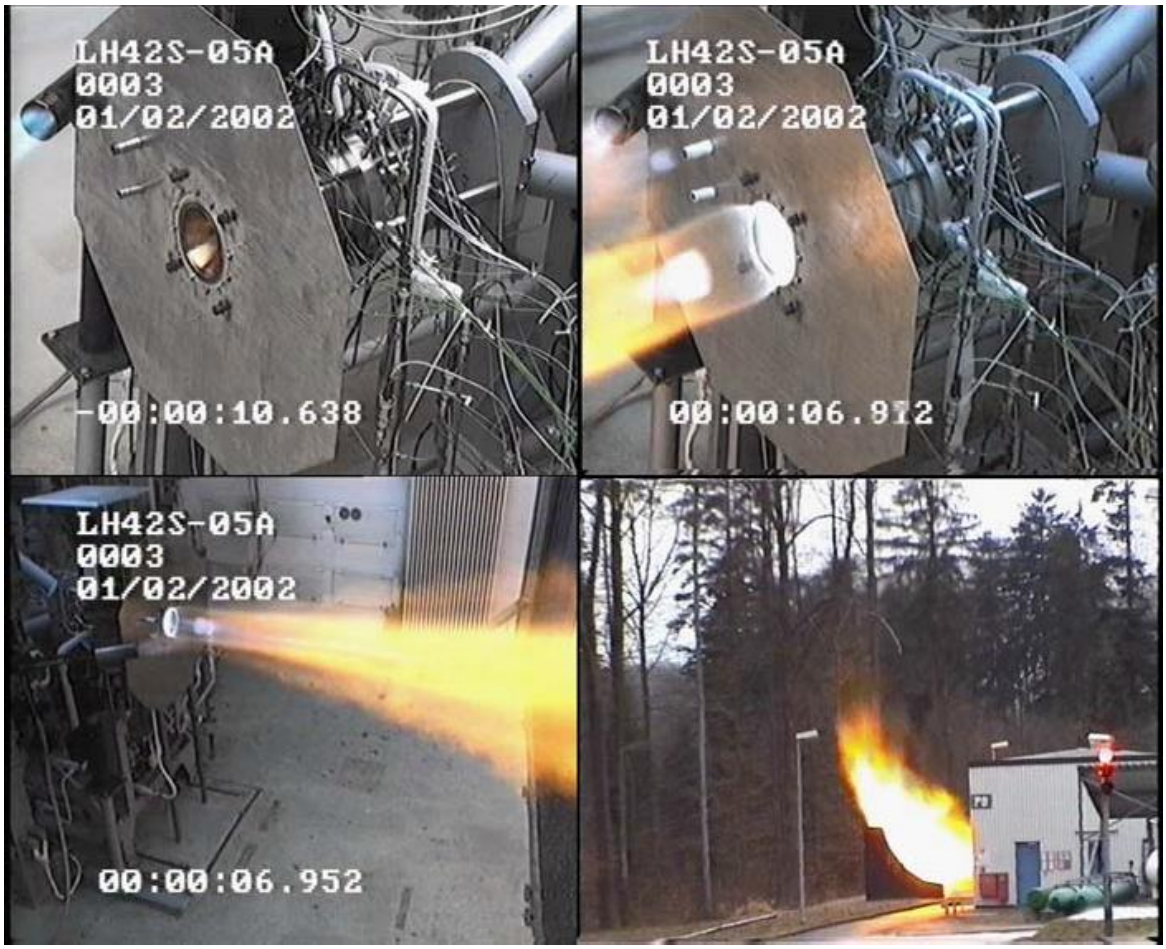

Figure 4.3. Test Bench P8 in action (DLR Institute of Space Propulsion, 2007)

4.2 Methodology

The test set up should be the same during all tests. Only those parts will be replaced that are necessary to complete the anticipated tests. Figure 4.4 depicts the basic test setup and is based on conducting the tests in Test Bench P8.1, using rocket engines developed and under test for the Lumen program, which program facilitates our experiments during their test runs. The central operations control room for P8 is located at building D68, and the operator in the control room will trigger the tests from there on our behalf.

Test process

The goal of the tests is to collect data from the sample plasma (6) in the rocket fume exhaust produced by the rocket engine (4) using a camera (9) that can collect and register the spectrum from and around the sample. The spectrum radiation is dispersed in two perpendicular or orthogonal directions and displayed in a two-dimensional pattern by the spectrograph (8) and captured by the camera (9), in one shot, with high spectral resolution and a broad wavelength range. The recorded pictures with the captured spectra are forwarded to the personal computer (10) for further processing after the test data collection.

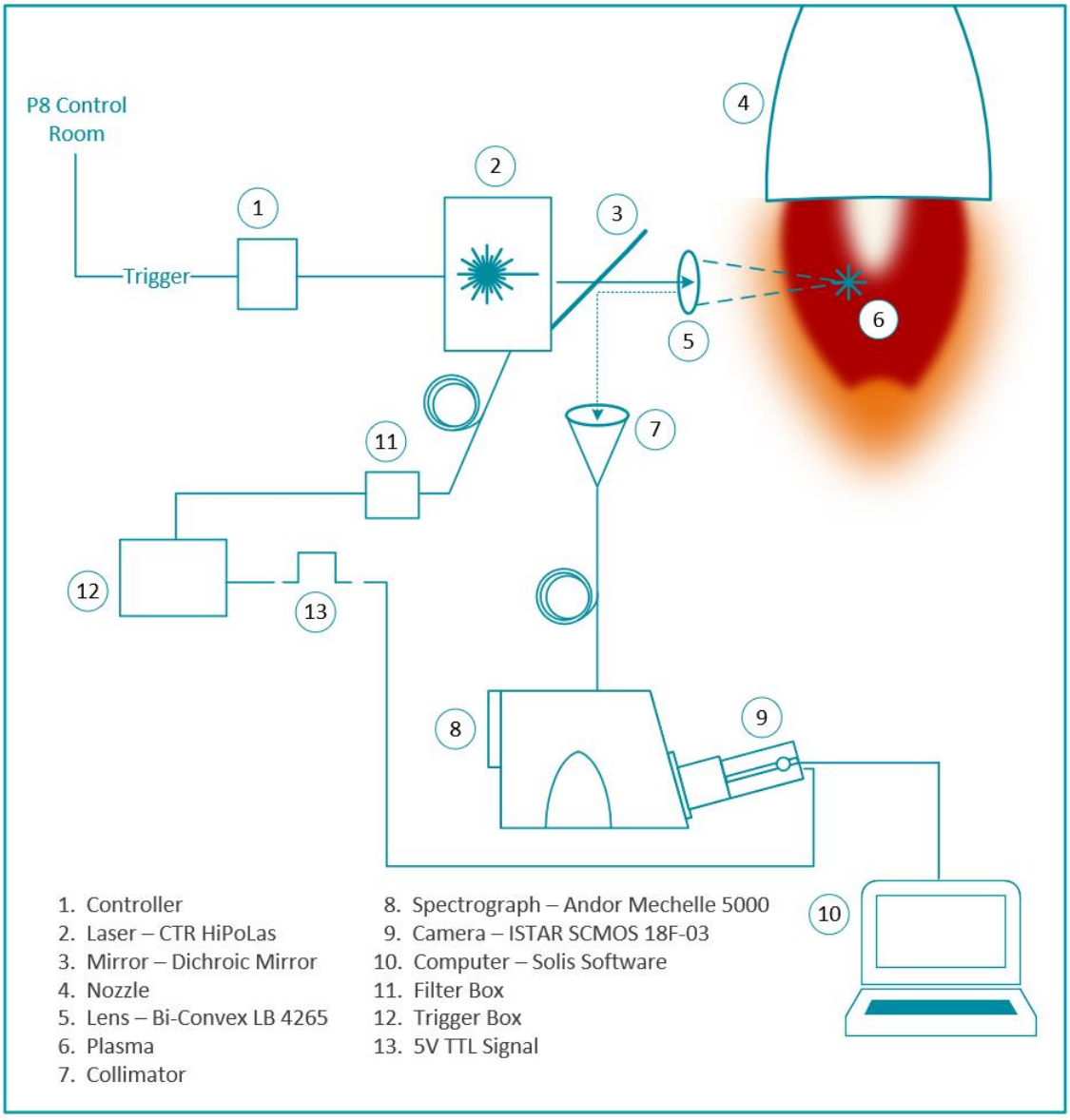

Figure 4.4. The basic test set up

As soon as the P8 Control Room pulls the test trigger (1), the laser (2) will send pulses of laser light. The laser beam transmits via the dichroic mirror (3) and focus lens (5), while laser light also transmits through a fiberglass cable to the filter box (11) that passes the wavelength used by the laser only, to a trigger box (12) that will trigger the camera (9) by sending a signal over 5V TTL (13) to ensure camera (9) and laser (2) are operating in sync.

After the laser light is transmitted and focused by focus lens (5) the laser light will hit matter at its focal point and induce plasma (6). The plasma, as it cools down, will emit photons at specific wavelengths typical for the hit elements. The emitted photons that hit the dichroic mirror (3) are reflected towards the collimator (7) and transmitted via fiberglass to the spectrograph (8) where a two-dimensional pattern as described above is generated and captured by the optical intensifiers of the camera (9) that convert the photons into electrons and sends the images to the personal computer (10).

Test procedure

The whole standard operating procedure for data collection, processing, evaluation, and reporting can be divided into 16 different steps, as shown in Figure 4.5

Figure 4.5. The 16-step standard operating procedure

Test plan

In this study, we want to prove feasibility incrementally. In test phase 1, the test will include testing the anticipated test set up end-to-end on location at the P8 Test bench to determine if the equipment will fit in the test facility and interfaces with the fixed infrastructure, like the UV-capable fiber optic cabling.

In test phase 1, the plasma will be generated from atmospheric air and captured using the spectrograph and the capturing camera (T1). The distance between the lens and the plasma will be in test phase 1 under 3 cm due to limitations of the setup.

In test phase 2, the distance will be increased up to 9 cm, and a flame from a Bunsen burner with an 80/20 butane/propane mixture of gas will emulate the rocket engines exhaust. In T2 plasma will be generated from the gas flame only. In T3 table salt will be added; in T4 Lithium; in T5 Copper; and in T6 scrap metal of unknown composition. T5 will be an ablative test.

In test phase 3, the plasma will be generated from matter in the exhaust of a rocket engine (T7). Testing with a rocket engine requires a certain safety distance for the focusing lens/telescope and collimator and possibly heat shielding.

Table 4.1. Overview of the test plan

Test #	Test description	Primary elements	Secondary elements
T1	Atmospheric Air Plasma	N, O, Ar	He, H, C
T2	80 Butane/ 20 Propane Flame	H, C, O	N, Ar, Fe, Cu
T3	Flame with Table Salt	Na, Cl, I, H, C, O	N, Ar, Fe, Cu
T4	Flame with Lithium	Li, H, C, O	N, Ar, Fe, Cu
T5	Flame with Eurocent (ablative)	Cu, H, C, O	N, Ar, Fe, (Cr, Mn, V, Mo)
T6	Flame with Scrap Metal	Fe, ??, ??, H, C, O	N, Ar, Fe, Cu
T7	Rocket Engine Exhaust Plume	H, C, O, Fe	TBD

4.3 Equipment

Although the Dutch technology provider pulled out of the project, resulting in needing to find a replacement for almost 80% of the required equipment, an inventory scan at the DLR Institute of Space Propulsion enabled us to instigate the first test round in Test Bench P8. Additional focus equipment was ordered for the following tests. The laser used during the first test (Test 1A) stopped working, and the second test (Test 1B) could not be concluded with it. This laser was out of order ever since. An alternative laser was not compatible with the other equipment in the test set up; fortunately, the supplier of that laser was willing to provide a compatible one. The size and weight of this new laser and that of the power supply make them not suitable as a smart sensor onboard a rocket but suffice for the next round of tests.

Laser 1 – CTR HiPoLas

The Carinthian Tech Research High-Power-Laser (HiPoLas) used was a class 4, monolithic, diode-side pumped, passively Q-switched Nd-YAG laser. Nd:YAG lasers are solid-state lasers that use an Nd:YAG (Neodymium-doped Yttrium Aluminum Garnet) crystal rod to produce the laser light. Nd:YAG lasers produce photons with a wavelength of 1064 nm. The HiPoLas provides peak energies up to 33.2 mJ at pulse durations of less than two nanoseconds with burst repetition rates of up to 100 Hz and is developed as an igniter in an upper stage cryogenic rocket combustor (Börner and Kroupa, 2018).

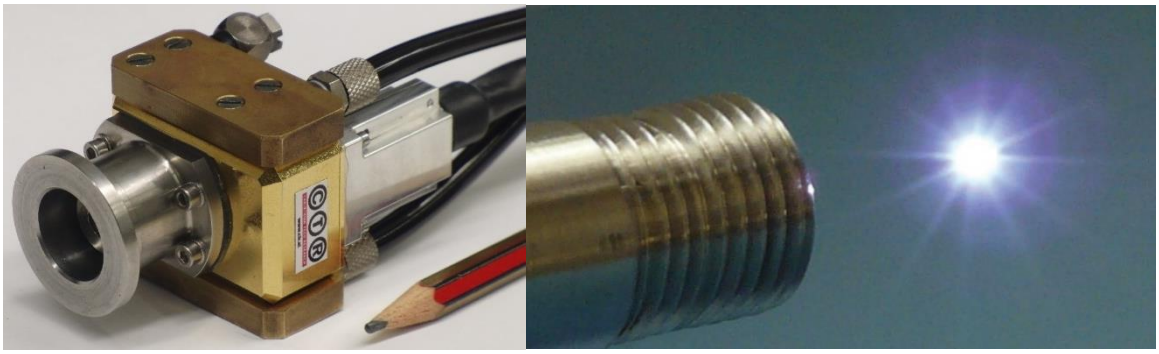

Figure 4.6. The Q-switched Nd-YAG laser (Baumgart, Glassl and Kroupa, 2011)

Laser 2 – Quantel Q-smart 850

The Lumibird Quantel Q-smart 850 laser was used after the HiPoLas unexpectedly stopped working. The Quantel 850 is also a 1064nm Nd:YAG laser with a slower repetition rate of 10 Hz., however, significantly more power with peak energies up to 850 mJ, a pulse duration of ~6ns, and passive and active Q-switching. The additional power and cooling needs make this laser with a head of 7 kg and a power supply of 27 kg, both without coolant weight, too bulky to integrate into a rocket propulsion system (Quantel, 2013). For in-lab and Test Bench testing it will suffice.

Figure 4.7. Quantel Q-smart 850 laser head and touch screen control panel (Quantel Laser, 2013)

Spectrograph – Andor Mechelle 5000

The Andor Mechelle 5000 is a spectrograph based on echelle diffraction grating and uses a patented dispersion balanced order sorting system that distributes the spectral order uniformly in contrast to other echelle spectrographs, optimizing CCD efficiency and achieving large bandwidth easily. The Mechelle ME5000 uses a 52.13 line/mm grating blazed at 32.35° and to achieve the best resolution; two custom-made correction lenses are used. Other components of the device are an entrance and exit window, a field-correcting lens made of CaF2, and two prisms to realize semi-equal order spacing. An optional collector and aiming laser can be used and connected via fiber. The laser can be

coupled to the fiber, and the light exiting the detector can be used to adjust focus and orientation.

The Mechelle covers a wavelength range from 200 to 975 nm without gaps in a single acquisition with a resolution power up to 6,000 nm. If a shorter wavelength detector is used, this range will be reduced accordingly. A spectral calibration source is needed to wavelength calibrate the Mechelle. Andor recommends using a mercury or argon lamp for calibration. To operate the Mechelle software is required; this can either be the Mechelle SDK or Solis for Spectroscopy.

The diffraction grating type echelle uses many slits with sizes almost matching the wavelength of the diffracted light. By using two dispersion stages, the echelle spectrograph disperses the received light in two perpendicular or orthogonal directions providing high spectral resolution and large spectral bandpass at the same time. The spectral data is displayed in a two-dimensional pattern which can be detected using a CCD or CMOS camera. The main benefit of Echelle spectrographs is the ability to measure both high spectral resolution and a broad wavelength range in one shot. However, a relatively low light sensitivity makes it necessary to use image intensifiers, which, on the other hand, can be used as high-precision gaters. (Andor, n.d.a).

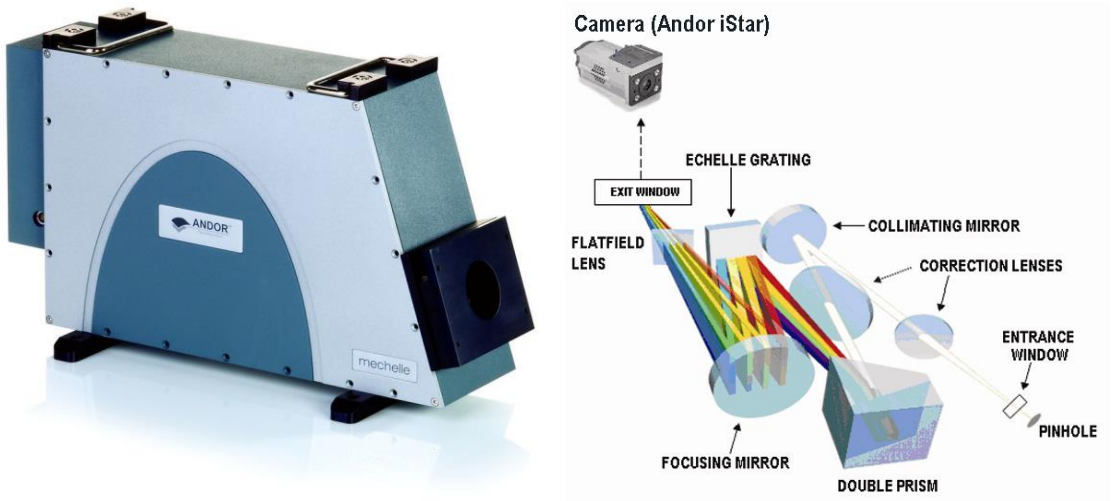

Figure 4.8. Andor Mechelle 5000 Spectrograph (Andor, n.d.c)

Camera – ISTAR-SCMOS 18F-03

The ISTAR-SCMOS 18F-03 camera was used as the capturing device. This camera is based on a front-illuminated scientific Complementary Metal-Oxide Semiconductor (sCMOS) image sensor to convert light into electrons warranting superfast frame rate capabilities of > 40 fps and nanosecond gating of < 2 ns. LIBS plasmas typically have a 1-100µs lifetime making expensive ICCD based cameras overkill.

The used camera type was configured with an intensifier diameter of Ø 18 mm, a fast gating speed, and a Gen 2 W-AGT photocathode, P43 phosphor as image intensifier supporting a wavelength range of 180 - 850 nm. Frame rates up to 50 fps (4,000 with ROI) using a USB 3.0 interface with UASP are supported.
The main benefits of sCMOS are the attainable high readout speeds, its low power consumption, and the price. Downsides are the lower light sensitivity (photons hitting the transistors and not the photodiode) and the susceptibility to noise.

To operate the camera software is required; this can be the Solis for Time-Resolved, Andor SDK3, or Andor GPU Express (Andor, n.d.b) The SDK provides an API for system integration purposes.

Mirror System – Thorlabs DMLP950 Dichroic Mirror

The Thorlabs DMLP950 - Ø1" Longpass Dichroic Mirror, 950 nm Cut-On was used to transmit the laser light towards the sample while the returning emission light was reflected by the mirror.
A dichroic mirror separates light spectrally by transmitting and reflecting light as a function of wavelength. For a longpass dichroic mirror, the transmission and reflection band are divided by a cut-on wavelength and is therefore highly transmissive above the cut-on wavelength and highly reflective below it. On one side, the dichroic mirror has a dichroic coating and on the other side, an anti-reflection coating. It should be used with a 45° angle of incidence (Thorlabs, 2014).

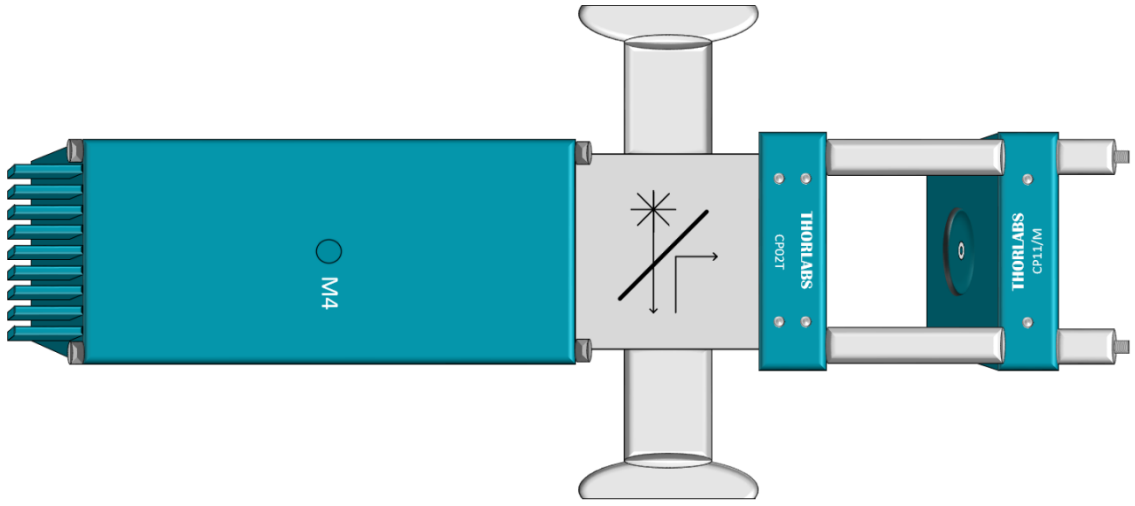

Figure 4.9. Thorlabs Dichroic Mirror Mounting Frame

Focus Lens – Sapphire Spherical Plano-Convex Lens

Sapphire (Al2O3) Plano-Convex lenses have an extremely hardness, are chemically inert, can be used with high temperatures up to 1,000 °C, and is a transparent focusing optic between 150 nm and 4.5 µm. Plan-Convex lenses are used for focusing a collimated beam or collimating a point source.

Focus Lens – Thorlabs Bi-Convex LB 4265

This lens, with the specifications f = 150.0 mm, Ø1" UV fused silica bi-convex lens, uncoated is used to focus the laser beam on the sample. This lens displays no laser-induced fluorescence and is ideal for application in UV, visible light, and NIR spectrum. (Thorlabs, 2000).

Bunsen Burner – Campingaz LABOGAZ 206

The Bunsen burner used in the experiments is using disposable canisters with a compressed mixture of Butane and Propane gas with a ratio of 80/20 Butane/Propane, typical for the brand Campingaz (Lab Unlimited, n.d.). Butane is an easy liquefiable gas and derived from fossil sources, petroleum in particular, as well as propane. The part of the Bunsen burner that's continuously affected by the flame, the rech burner, is made of at least two types of metal, these elements might show up in samples due to wear debris of the rech burner.

NIST Database

The National Institute of Standards and Technology (NIST), part of the United States Federal Department of Commerce, is a combination of six science laboratories and is among others, responsible for measurements standards, material measurement, and physical measurement.

The NIST Physical Measurement Laboratory (PML) runs an Atomic Spectra Database (ASD) for energy levels and radiative transitions in atoms and atomic ions. For most known chemical elements, the database includes information of observed transitions and energy levels, spectral lines with wavelengths from about 20 picometers to 60 meters, as well as for many lines the radiative transition probabilities.

The ASD is publicly accessible via a webpage interface but also via an Application Programming Interface (API). The database provides a dedicated interface for LIBS applications that can be used to compare collected experimental data with synthetic plots based on ASD data (NIST, 2018). Other databases with publicly available spectral data are AtomTrace (Czech Republic) and Kurucz (Harvard).

The synthetic plot provides a graph with the wavelengths and line intensity, which are unique for every element or composition and can be considered a "fingerprint." This

synthetic fingerprint and can be compared to the actual fingerprint captured using a spectroscope and capturing camera.

The ASD can be found at https://www.nist.gov/pml/atomic-spectra-database

The figures 4.10, 4.11, 4.12, and 4.13 illustrate the Synthetic Fingerprints as generated using ASD data for the most abundant element in the universe (H, Hydrogen) and the three main constituents of the earth's atmosphere at sea level (N, Nitrogen | O, Oxygen | Ar, Argon).

Looking at a couple of frames that captured the signatures of all these elements, one would almost think that Argon is the most abundant element in the composition, this is caused by the abundance of spectral lines photons emitted by Argon create. From 300nm to 850nm Argon has 1,561 spectral lines and Hydrogen only 182; intensity, ionization level, and Einstein's Coefficient are other influencing factors.

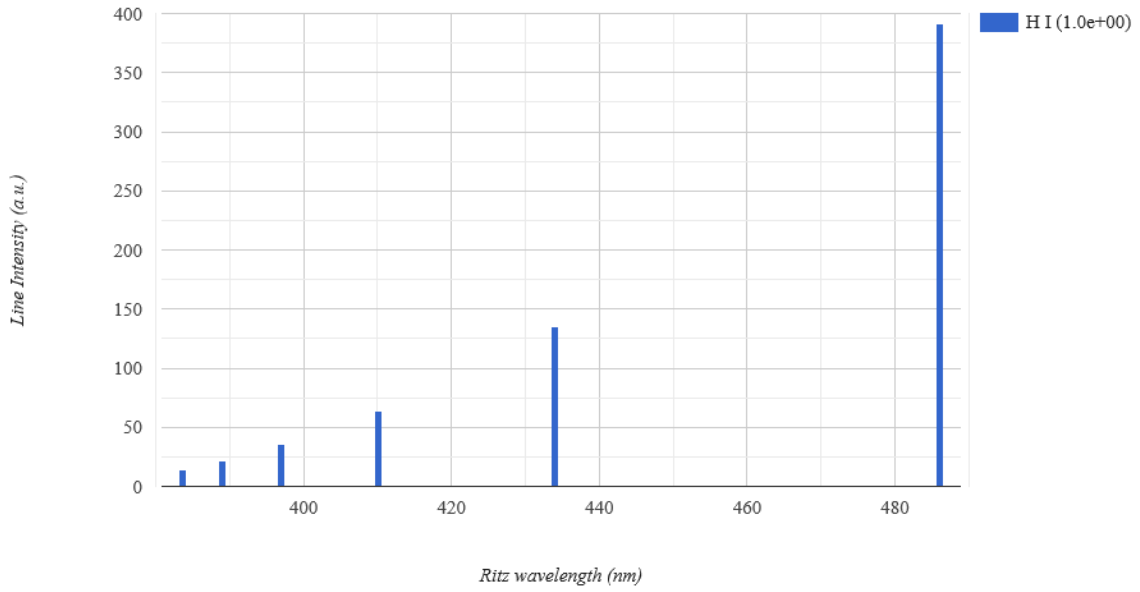

Figure 4.10. ASD Synthetic Fingerprint of Hydrogen between 200 and 500 nm (NIST, 2018)

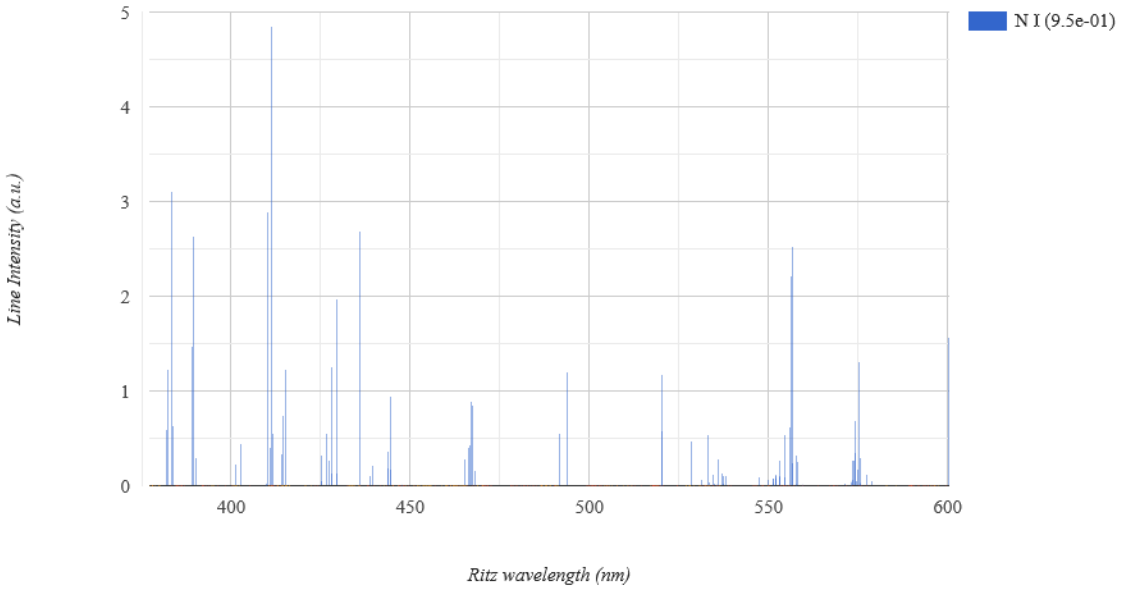

Figure 4.11. ASD Synthetic Fingerprint of Nitrogen between 375 and 600 nm (NIST, 2018)

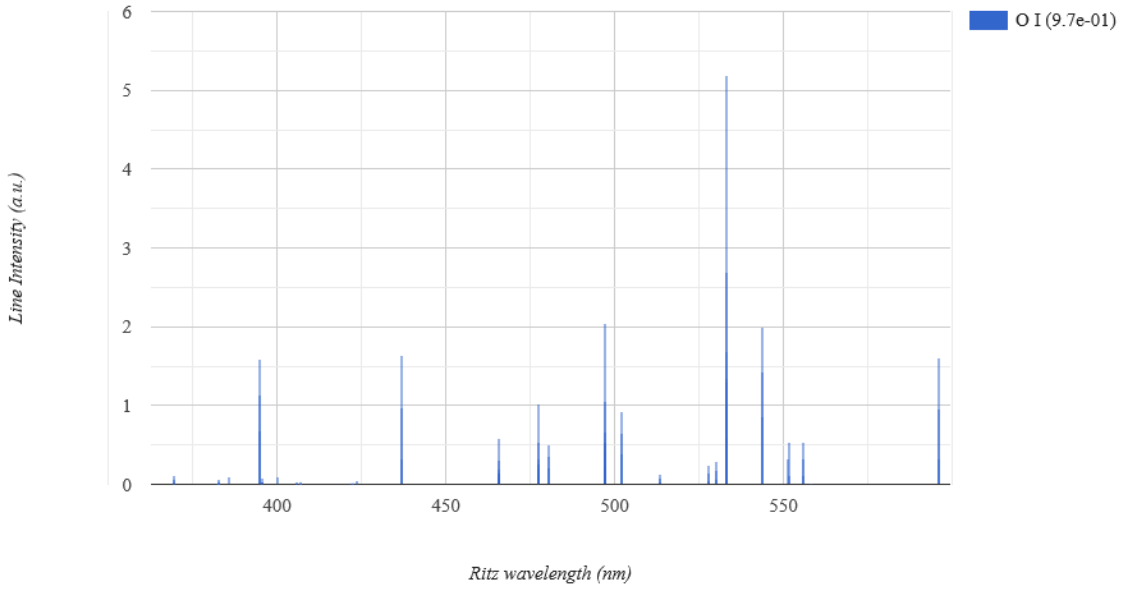

Figure 4.12. ASD Synthetic Fingerprint of Oxygen between 200 and 600 nm (NIST, 2018)

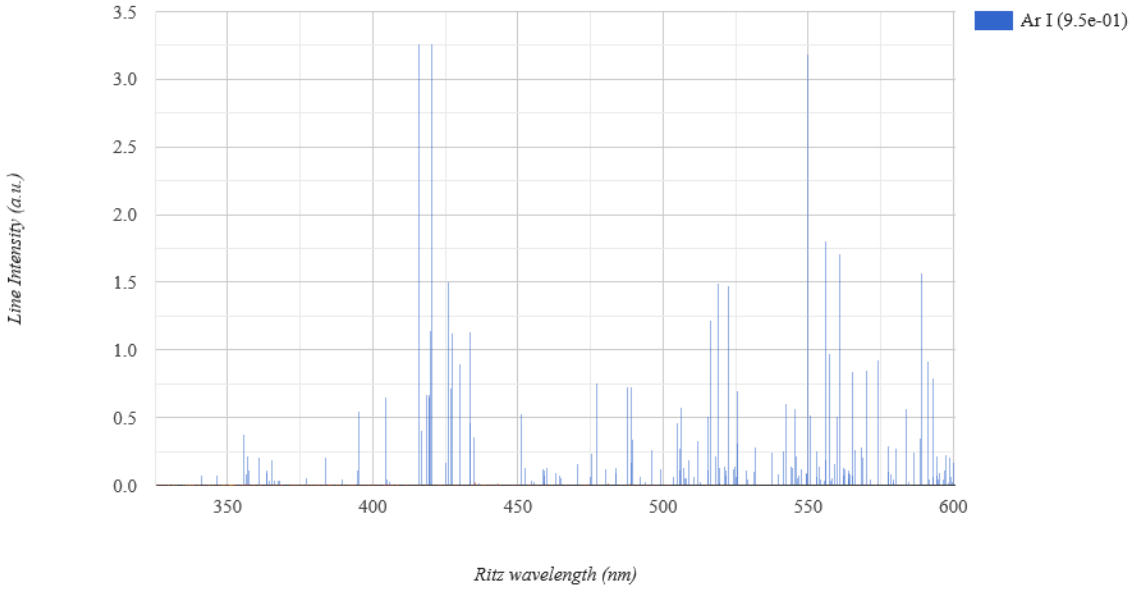

Figure 4.13. ASD Synthetic Fingerprint of Argon between 325 and 600 nm (NIST, 2018)

Analytics Software

Andor Solis

Andor Solis is an acquisition, display and processing software for use with Andor Spectroscopes and Andor iStar cameras. There are multiple versions to support multiple application types. Solis-I focuses on Imaging, Solis-S on Spectroscopy, and Solis-T on time-resolved fast gating.

The Andor Solis software can be used instead of the SDK that comes with the Andor spectroscope or camera. Before using the devices and tool, calibration is needed. If not calibrated orderly, the results might be invalid, and the presented results can be incorrect. Data can be exported in different data sets allowing the user to use different tools to analyze the data. Solis provides diagrams and has the potential for automated identification of elements based on spectral lines (Andor Solis, N.D.).

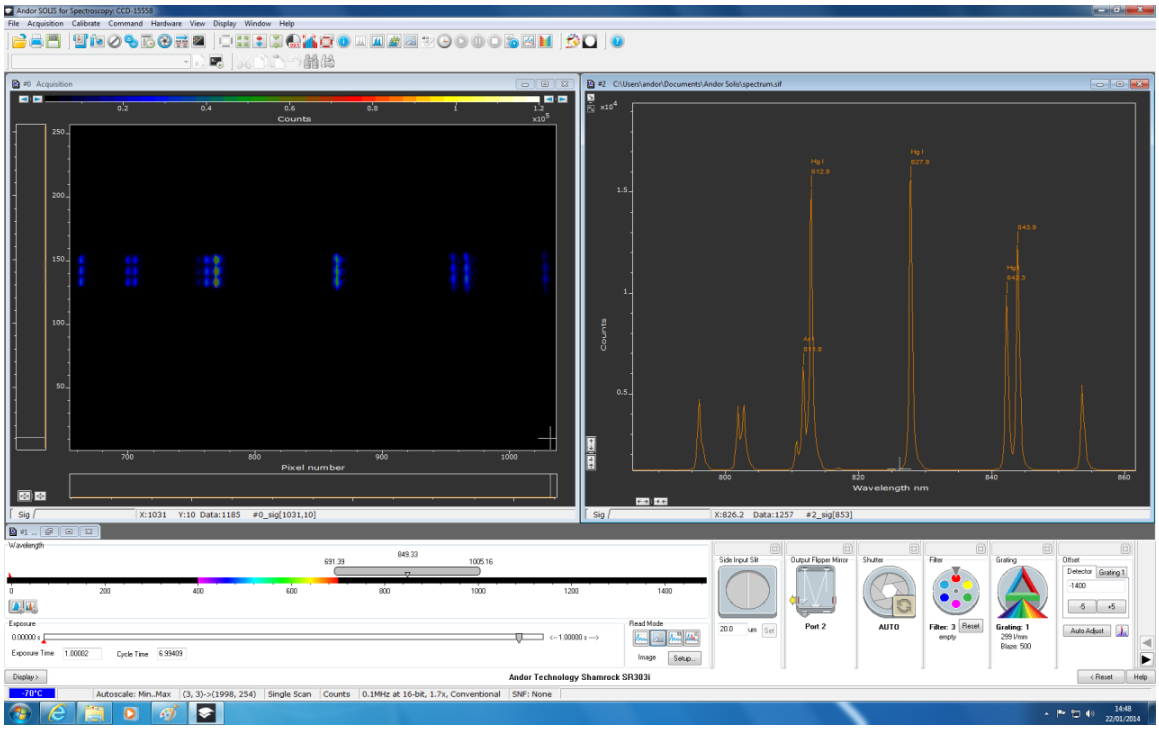

Figure 4.14. Andor Solis-T User Interface for Time-Resolved Imaging (Andor Solis, n.d.)

Origin

Origin is a data analysis and graphing software toolset for engineers and scientists made by Origin Lab. The creation of high-quality graphs in a short period is a significant strength of Origin. The many features and capabilities of the software can be overwhelming for a first-time user. At DLR, the older 8.1 version (2009) is used, which has some difficulties displaying multiple layers of data. The current version 2019b handles multiple layers without any issues.

Origin provides interfaces to other applications like MATLAB, LabVIEW, and Microsoft Excel. Custom code can be created within Origin using Origin scripting or a programming language; a library of 100 graph types is standard available, and all elements are customizable. Over 30 different file formats are supported, and data from other sources can be accessed using data connectors, and graphs can be exported as graphics in more than 15 file formats (OriginLab, n.d.).

Origin will be used to generate high-quality graphs that cannot be created using the Andor Solis software to analyze data and to visualize the final results of this study.

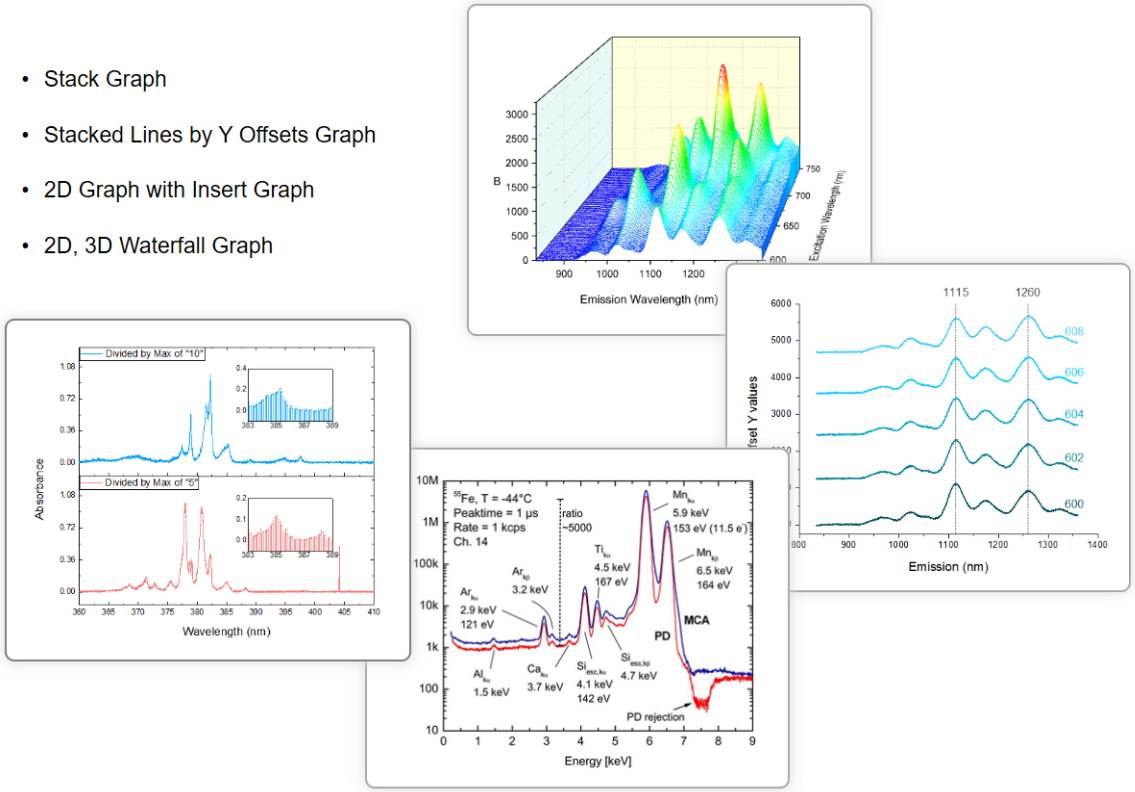

Figure 4.15. Origin Plot Type Samples for Spectroscopy (OriginLab, n.d.)

5. Results and Discussion

The laser break-down and belated replacement required adapting the test plan. Test 1 has been repeated in test facility M3 with the new laser (T1b). The last rocket-engine test took place on July 16th, but no suitable laser was available at the time, resulting in postponing T7 till after the release deadline of this report. Table 5.1 Lists the actual tests performed.

Table 5.1. Actual tests performed

Test #	Test description	Primary elements	Secondary elements
T1a	Atmospheric Air Plasma	N, O, Ar	He, H, C
T1b	Atmospheric Air Plasma	N, O, Ar	He, H, C
T2	80 Butane/ 20 Propane Flame	H, C, O	N, Ar, Fe, Cu
T3	Flame with Table Salt	Na, Cl, I, H, C, O	N, Ar, Fe, Cu
T4	Flame with Lithium	Li, H, C, O	N, Ar, Fe, Cu
T5	Flame with Eurocent (ablative)	Cu, H, C, O	N, Ar, Fe, (Cr, Mn, V, Mo)
T6	Flame with Scrap Metal	Fe, ??, ??, ??, H, C, O	N, Ar, Fe, Cu

5.1 Test 1a Air Plasma

In test T1a, the plasma was generated from atmospheric air. The distance between the lens and the plasma was under 3 cm. The test was executed in Test Bench P8.1. The difference with the basic test setup was the use of another lens (Sapphire lens) and the absence of a rocket-engine exhaust plume, see figure 5.1.

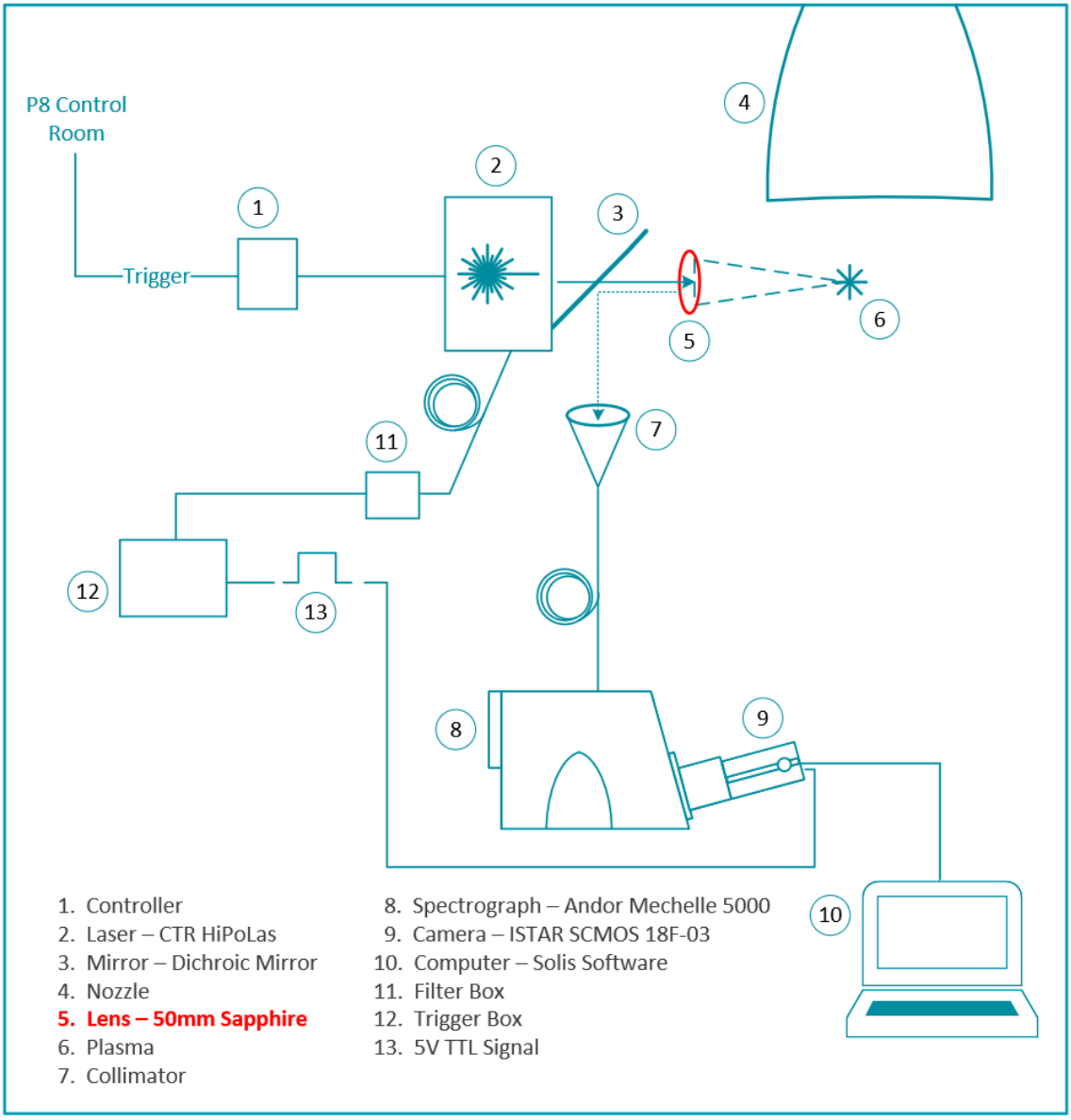

Figure 5.1. During Test 1a, a 50mm Sapphire lens was used, and no rocket-engine exhaust plume

Table 5.2 lists all elements that are present in the test under primary elements and other elements that are most likely present in the air as well under secondary elements. Figure 5.3 is the graph plotted using the sanitized data set. Table 5.3 provides an overview of the

test quality, observations, and conclusions. The data were analyzed for the three main elements in atmospheric air at sea-level, i.e., Nitrogen, Oxygen, and Argon only.

Table 5.2 T1a test overview

Test #	Test description	Primary elements	Secondary elements
T1a	Atmospheric Air Plasma	N, O, Ar	He, H, C

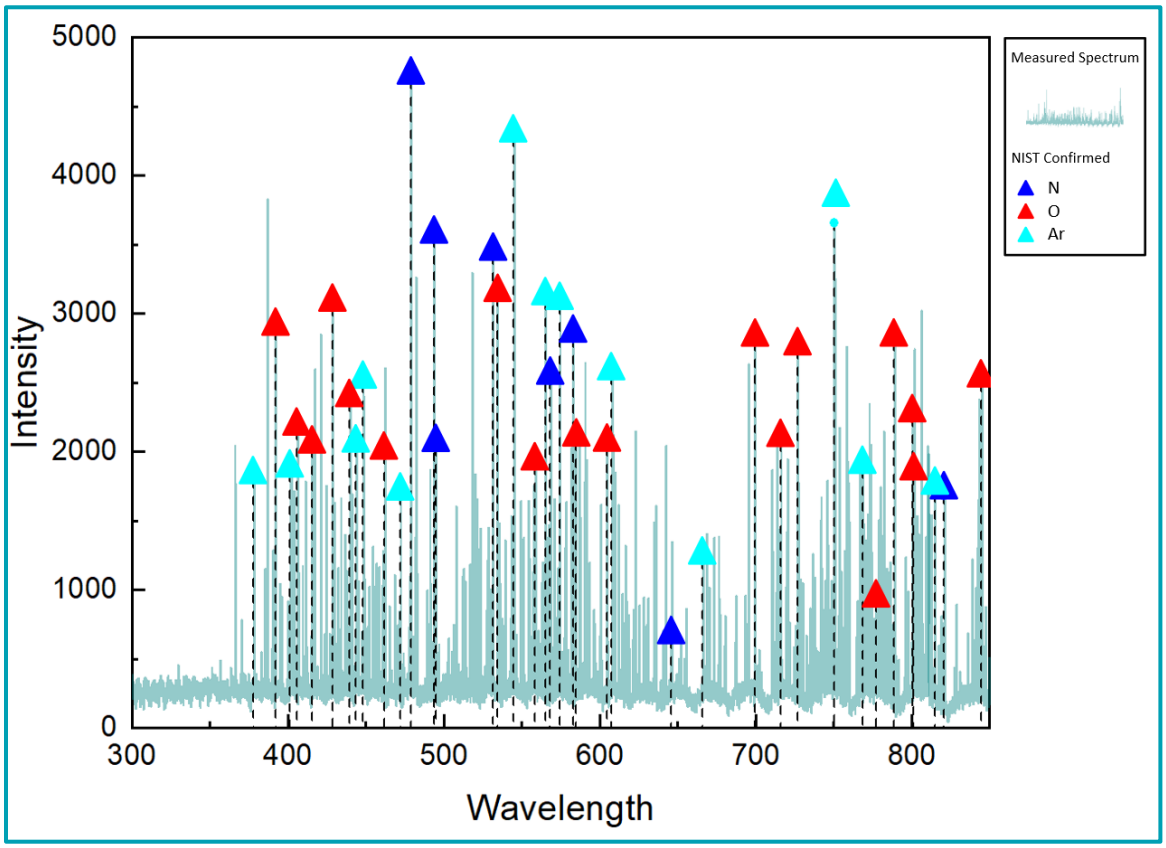

Figure 5.2. Chart showing sanitized data set of T1a with NIST confirmation where applicable

Table 5.3. Test results, observations and conclusions

Test ID	T1a Atmospheric Air Plasma
Test type	Non-ablative
Capturing data successful	Yes
No. of frames captured	90 frames
Acceptable noise level	Yes
No. of spectral lines sufficient	Yes - Excellent intensity
Usable frames	Yes
NIST confirmation of findings – rating	Yes – Excellent

Sufficient spectral lines per element	Yes
Dataset plotting worthy	Yes
Patterns of all elements convincing	Yes

Observations

- The graph is coherent.
- The overall count intensity is excellent.
- The number of spectral lines per element is excellent.
- All spectral lines are confirmed by the NIST Atomic Spectra Database.
- The spectral lines indicate detection of H traces with a probability bordering on certainty.
- The spectral lines indicate detection of O traces with a probability bordering on certainty.
- The spectral lines indicate detection of Ar traces with a probability bordering on certainty.
- The spectrum signatures of all expected elements are all evidently visible.

Conclusions

- We can detect traces of H, O, and Ar in atmospheric air using LIBS.

5.2 Test 1b Air Plasma

In test T1b, the test done under T1a with plasma generated from atmospheric air was repeated with a new laser because the original laser used in T1a broke. The distance between the lens and the plasma was increased to almost 9 cm. The test was executed in test laboratory M3. The difference with the basic test setup was the use of another laser (Quantel Q-smart 850), the absence of a rocket-engine exhaust plume, and the use of a local trigger board See figure 5.3.

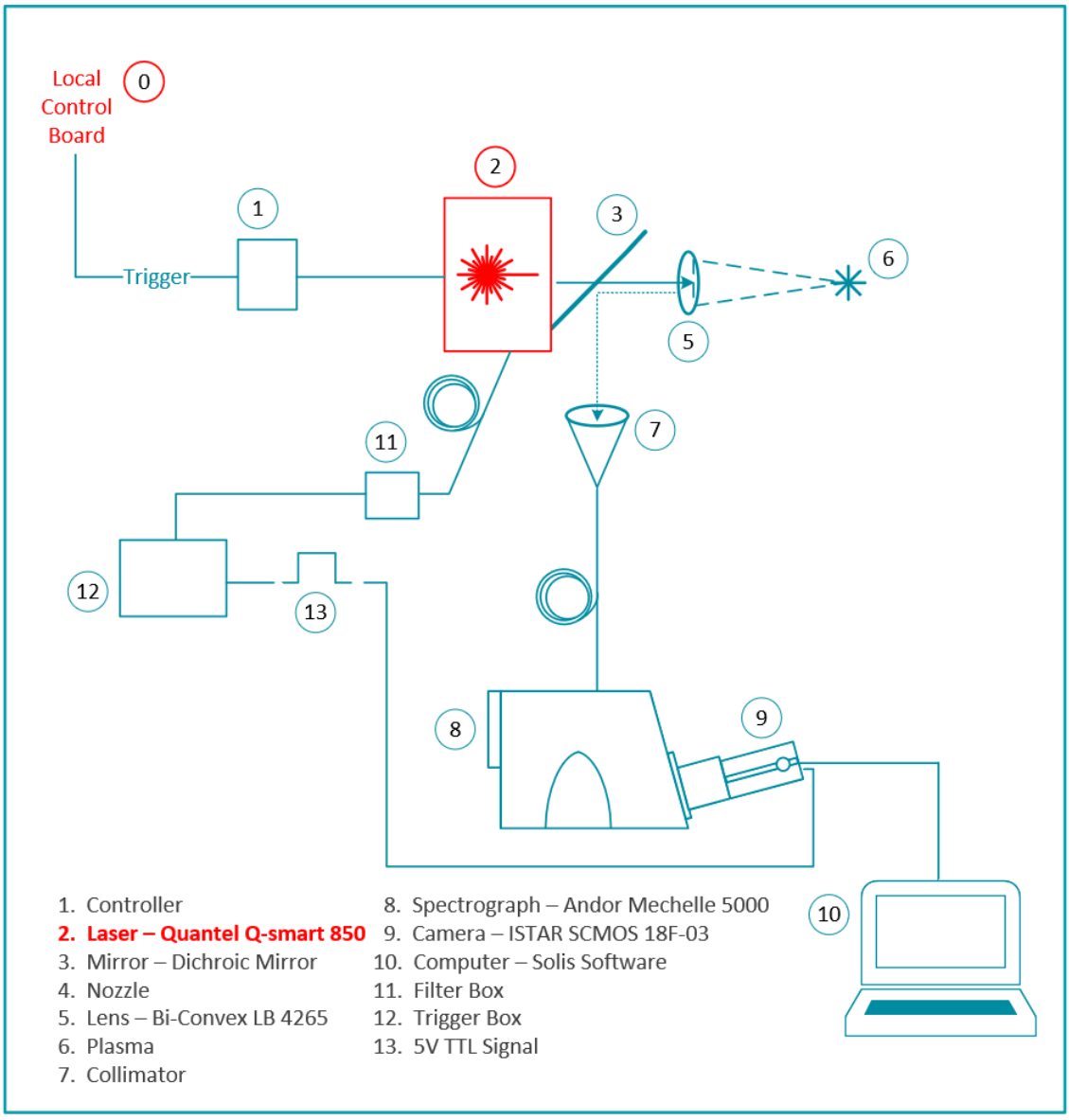

Figure 5.3. For Test 1b the laser was replaced by a Quantel Q-smart 850 and used an alternative triggering procedure

Table 5.4 lists all elements that are present in the test under primary elements and other elements that are most likely present in the air as well under secondary elements. Figure 5.3 is the graph plotted using the sanitized data set. Table 5.4 provides an overview of the test quality, observations, and conclusions. The data was analyzed for the three main elements in atmospheric air at sea-level, i.e., Nitrogen, Oxygen, and Argon only.

Table 5.4 T1b test overview

Test #	Test description	Expected elements	Present other elements
T1b	Atmospheric Air Plasma	N, O, Ar	He, H, C

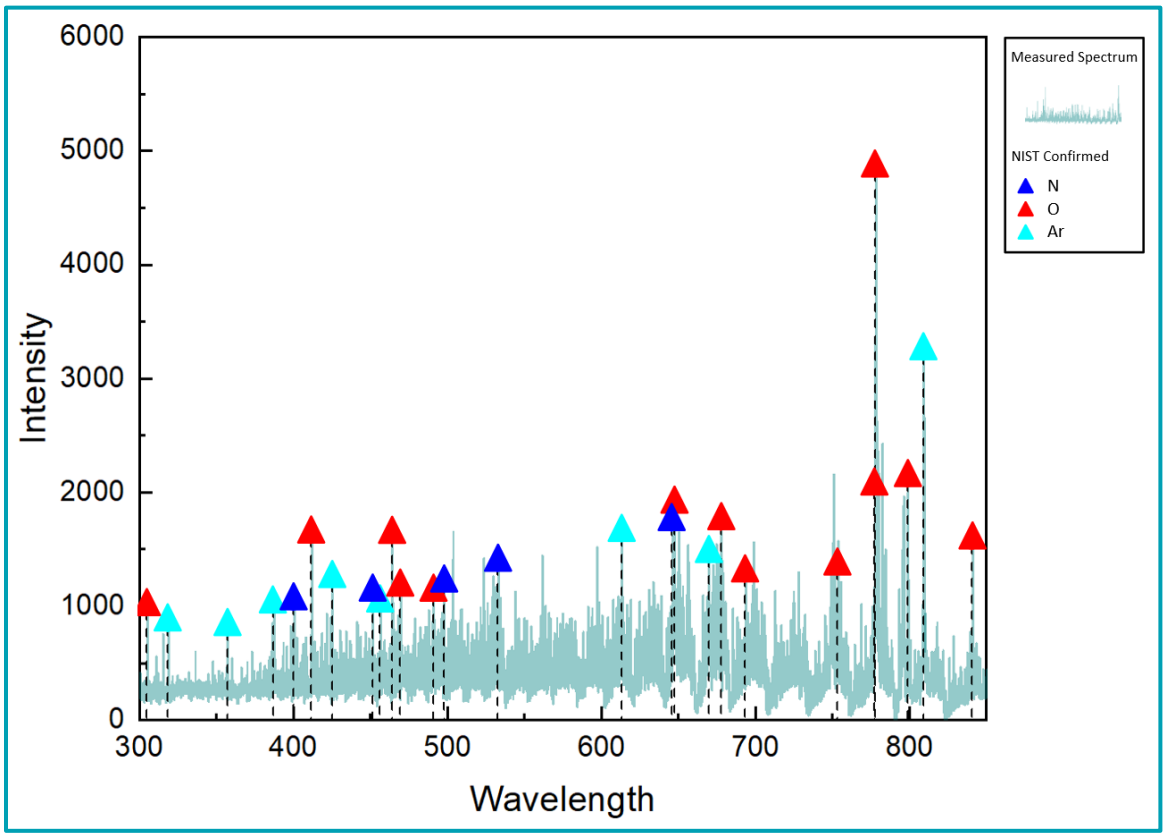

Figure 5.4. Chart showing sanitized data set of T1b because the original with NIST confirmation where applicable

Table 5.5. T1b test results, observations and conclusions

Test ID	T1b Atmospheric Air Plasma
Test type	Non-ablative
Capturing data successful	Yes
No. of frames captured	10 frames
Acceptable noise level	Yes
No. of spectral lines sufficient	Good
Usable frames	Yes
NIST confirmation of findings – rating	Yes – Excellent
Sufficient spectral lines per element	Yes
Dataset plotting worthy	Yes
Patterns of all elements convincing	Yes

Observations
- The graph is coherent. - The overall count intensity is good. - The number of spectral lines per element is good. - All spectral lines are confirmed by the NIST Atomic Spectra Database. - The spectral lines indicate detection of H traces with a probability bordering on certainty. - The spectral lines indicate detection of O traces with a probability bordering on certainty. - The spectral lines indicate detection of Ar traces with a probability bordering on certainty. - The spectrum signatures of all expected elements are all evidently visible.
Conclusions
- We can detect traces of H, O, and Ar in atmospheric air using LIBS.

5.3 Test 2 Flame Plasma

The T2 test set up will be used in T3-T6 as well. The difference with the basic test set up is that the Bunsen burner in the set up is producing a flame instead of a rocket-engine exhaust plume, the use of another laser (Quantel Q-smart 850), and the use of a local trigger board See figure 5.5.

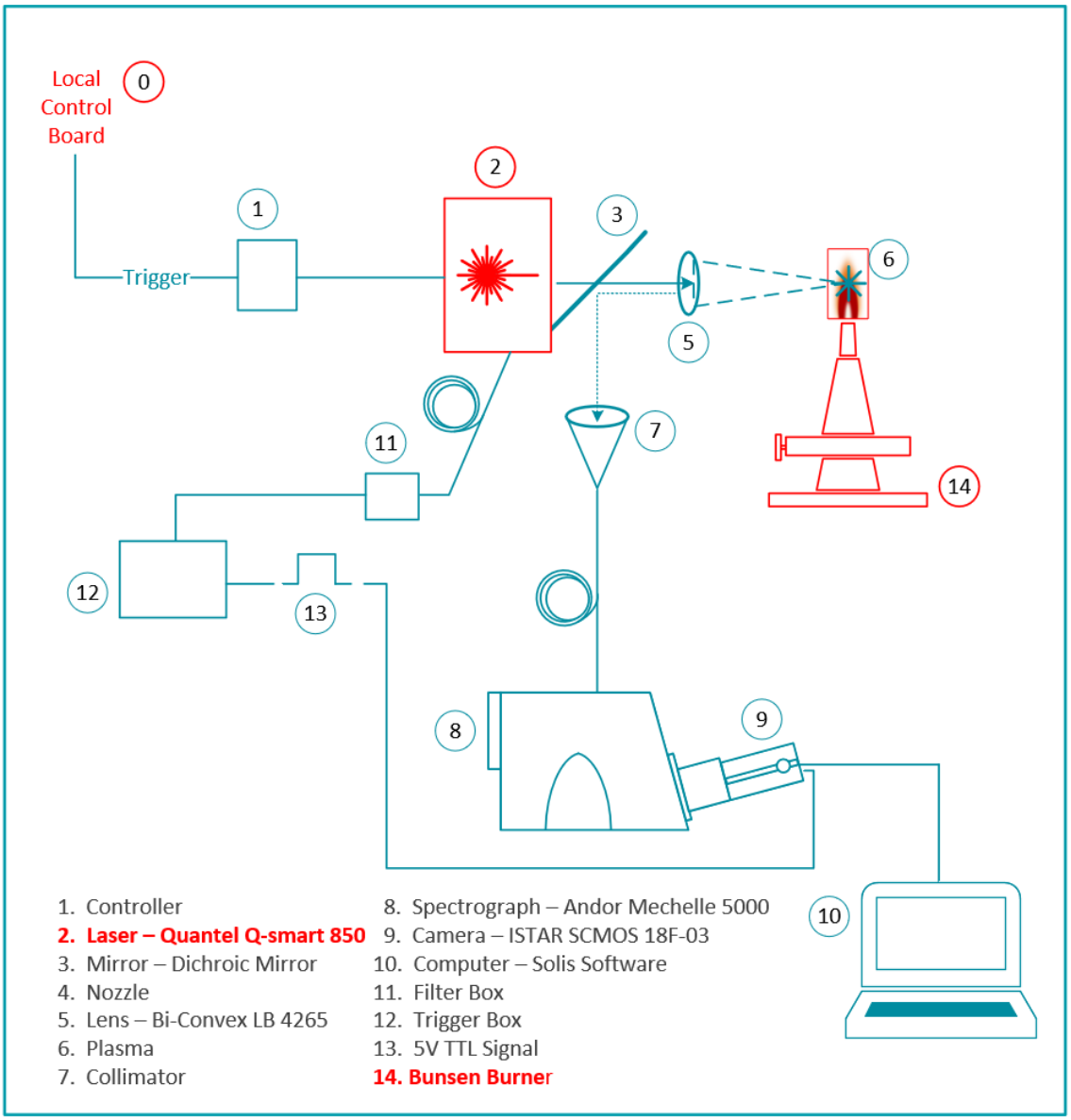

Figure 5.5. For tests T2-T6 the laser was replaced by a Quantel Q-smart 850, an alternative triggering procedure was used, and a Bunsen burner emulates the rocket-engine exhaust plume

In T2 plasma is induced inside a hydrocarbon flame (80% Butane and 20 % Propane) without any additives. The data were analyzed for the three main elements in the fossil fuel combustion process, i.e., Hydrogen, Carbon, and Oxygen.

Table 5.6 lists all elements that are present in the test under primary elements and other elements that are most likely present as well since they are in the surrounding air in possible wear debris from the burner under secondary elements. Figure 5.7 is the graph plotted using the sanitized data set. Table 5.7 provides an overview of the test quality, observations, and conclusions.

Table 5.6 T2 test overview

Test #	Test description	Expected elements	Present other elements
T2	80 Butane/ 20 Propane Flame	H, C, O	N, Ar, Fe, Cu

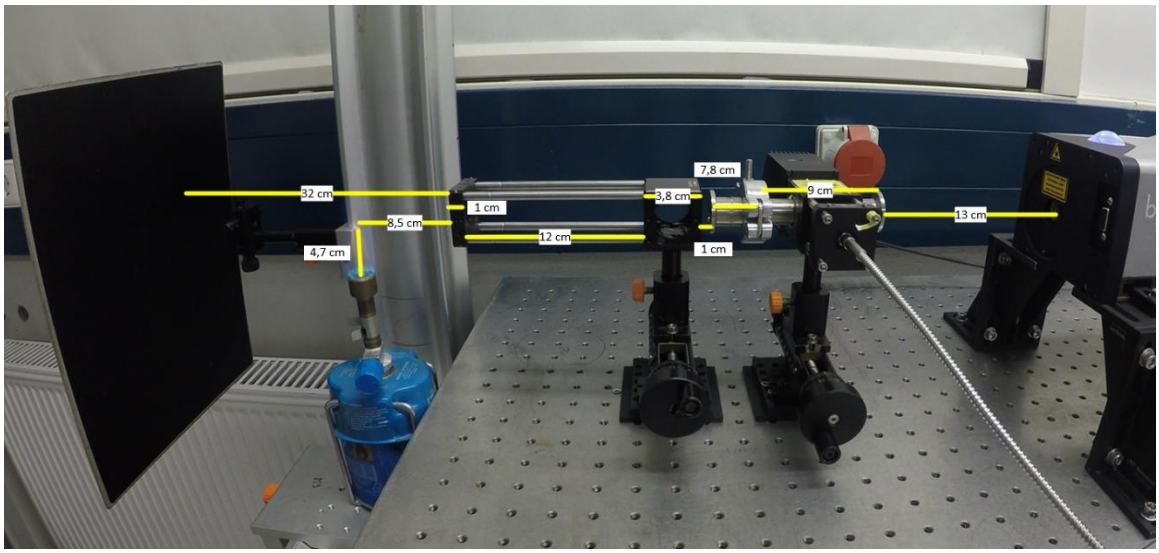

Figure 5.6. The test set up as used in tests T2-T6 with the applied distances

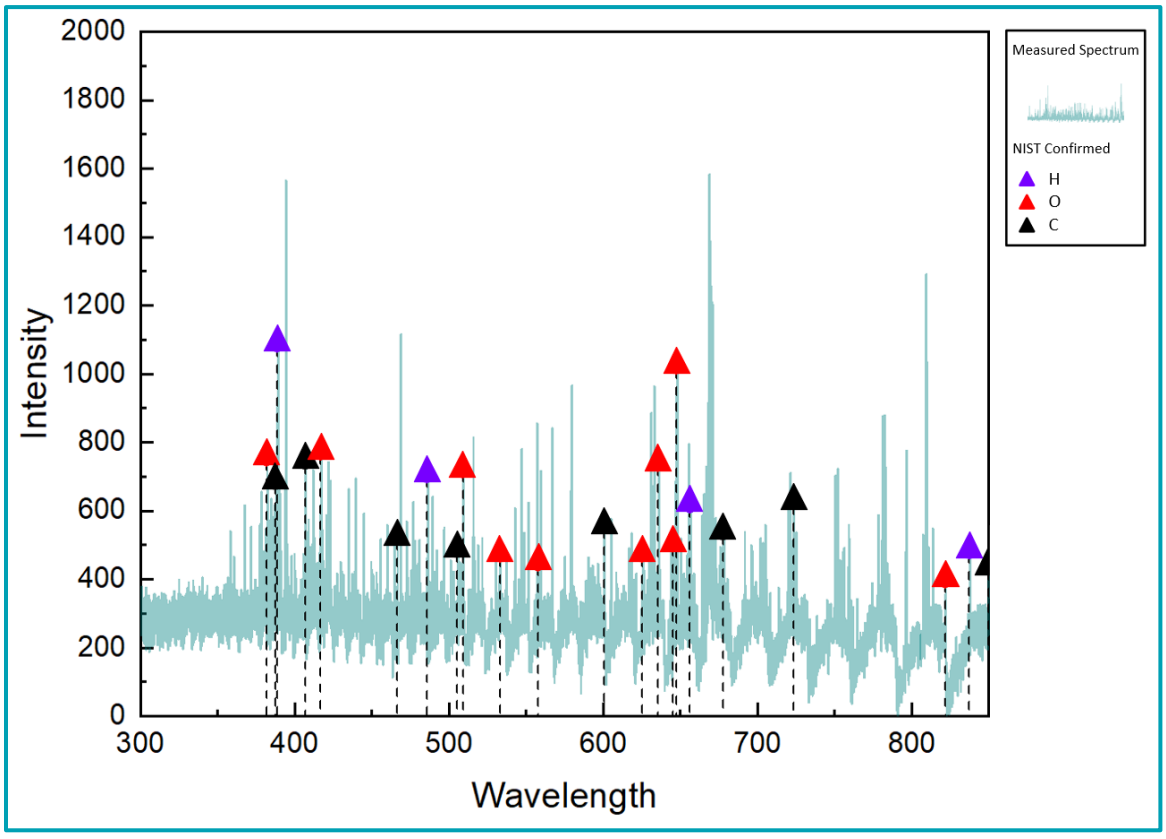

Figure 5.7. Chart showing sanitized data set of T2 with NIST confirmation where applicable

Table 5.7. T2 test results, observations and conclusions

Test ID	T2 80 Butane/ 20 Propane Flame
Test type	Non-ablative
Capturing data successful	Yes
No. of frames captured	100 frames
Acceptable noise level	Yes
No. of spectral lines sufficient	Yes
Usable frames	Yes
NIST confirmation of findings – rating	Yes – Excellent
Sufficient spectral lines per element	Yes
Dataset plotting worthy	Yes
Patterns of all elements convincing	Yes
Observations	
- The graph is coherent. - The overall count intensity is good. - The number of spectral lines per element is good. - All spectral lines are confirmed by the NIST Atomic Spectra Database. - The spectral lines indicate detection of H traces with a probability bordering on certainty. - The spectral lines indicate detection of C traces with a probability bordering on certainty. - The spectral lines indicate detection of O traces with a probability bordering on certainty. - The spectrum signatures of all expected elements are all evidently visible.	
Conclusions	
- We can detect traces of H, C, and O in a flame using LIBS.	

5.4 Test 3 Exhaust Plume Emulation 1

The T3 test set up was identical to the set up in test T2. A little amount of table salt was dispensed in the flame while measuring. The data were analyzed for the three main elements in table salt Sodium, Chlorine, and Iodine only.

Table 5.8 lists all elements that are present in the test under primary elements and other elements that are most likely present as well since they are in the surrounding air in possible wear debris from the burner under secondary elements. Figure 5.8 is the graph plotted using the sanitized data set. Table 5.9 provides an overview of the test quality, observations, and conclusions.

Table 5.8. T3 test overview

Test #	Test description	Primary elements	Secondary elements
T3	Flame with Table Salt	Na, Cl, I, H, C, O	N, Ar, Fe, Cu

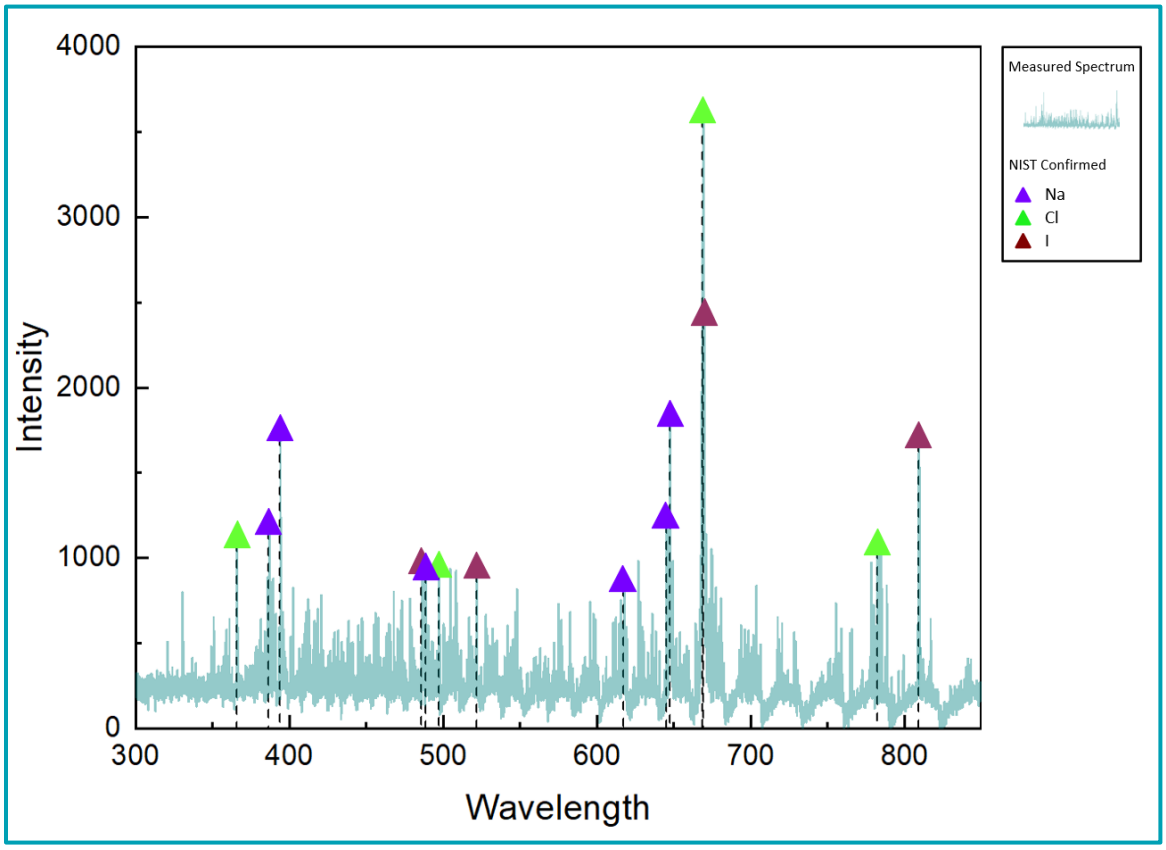

Figure 5.8. Chart showing sanitized data set of T3 with NIST confirmation where applicable

Table 5.9 T3 test results, observations and conclusions

Test ID	T3 table salt
Test type	Non-ablative
Capturing data successful	Yes
No. of frames captured	90 frames
Acceptable noise level	Yes, all frames
No. of spectral lines sufficient	Some frames. Low intensity

Usable frames	Yes
NIST confirmation of findings – rating	Yes – Excellent
Sufficient spectral lines per element	Yes
Dataset plotting worthy	Yes
Patterns of all elements convincing	Yes

Observations

- The graph is coherent.
- The overall count intensity is average.
- The number of spectral lines per element is good.
- All spectral lines are confirmed by the NIST Atomic Spectra Database.
- The spectral lines indicate detection of Na traces with a probability bordering on certainty.
- The spectral lines indicate detection of Cl traces with a probability bordering on certainty.
- The spectral lines indicate detection of I traces with a probability bordering on certainty.
- The spectrum signatures of all expected elements are all evidently visible.

Conclusions

- We can detect traces of Na, Cl and I in a flame using LIBS.

5.5 Test 4 Exhaust Plume Emulation 2

The T4 test set up was identical to the set up in test T2. A little amount of Lithium chlorine was dispensed in the flame while measuring. The data was analyzed for the main element Lithium only.

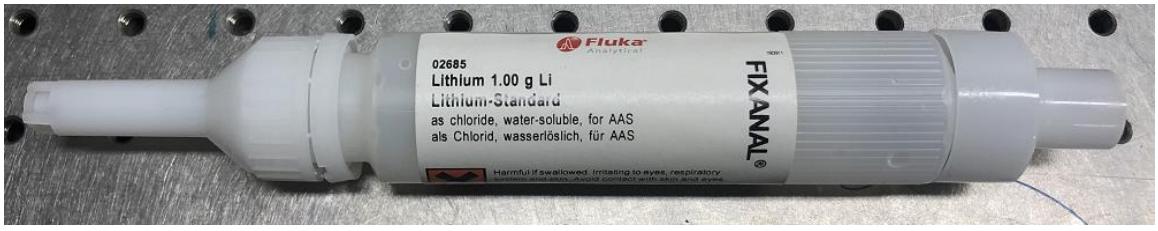

Figure 5.9. The sample of Lithium used in T4

Table 5.10 lists all elements that are present in the test under primary elements and other elements that are most likely present as well since they are in the surrounding air in possible wear debris from the burner under secondary elements. Figure 5.10 is the graph plotted using the sanitized data set. Table 5.11 provides an overview of the test quality, observations, and conclusions.

Table 5.10. T4 test overview

Test #	Test description	Primary elements	Secondary elements
T4	Flame with Lithium	Li, H, C, O	N, Ar, Fe, Cu

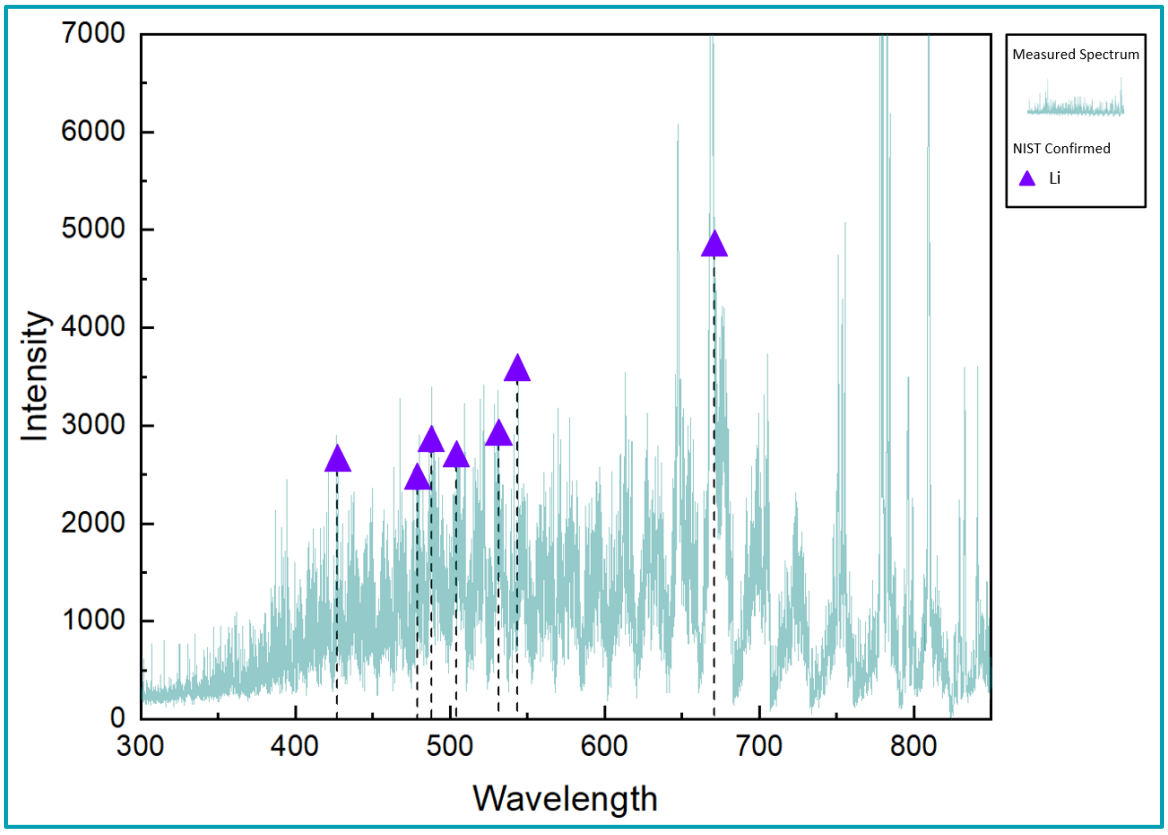

Figure 5.10. Chart showing sanitized data set of T4 with NIST confirmation where applicable

Table 5.11. T4 test results, observations and conclusions

Test ID	T4 flame with Lithium
Test type	Non-ablative
Capturing data successful	Yes
No. of frames captured	100 frames
Acceptable noise level	No, some average frames

No. of spectral lines sufficient	Some frames. Low intensity
Usable frames	Yes
NIST confirmation of findings – rating	Yes – Excellent
Sufficient spectral lines per element	Yes
Dataset plotting worthy	Yes
Patterns of all elements convincing	Yes

Observations

- The graph is coherent.
- The overall count intensity is average.
- The number of spectral lines is good.
- All spectral lines are confirmed by the NIST Atomic Spectra Database.
- The spectral lines indicate detection of Li traces with a probability bordering on certainty.
- The spectrum signature of the element is evidently visible.

Conclusions

- We can detect traces of Li in a flame using LIBS.

5.6 Test 5 Exhaust Plume Emulation 3

The T5 test set up was identical to the set up in test T2. A Eurocent coin was positioned in the flame while measuring. The data was analyzed for the main element of the coin cover Copper only.

Table 5.12 lists all elements that are present in the test under primary elements and other elements that are most likely present as well since they are in the surrounding air in possible wear debris from the burner under secondary elements. Figure 5.11 is the graph plotted using the sanitized data set. Table 5.2 provides an overview of the test quality, observations, and conclusions.

Table 5.12. T5 test overview

Test #	Test description	Primary elements	Secondary elements
T5	Flame with Eurocent (ablative)	Cu, H, C, O	N, Ar, Fe, (Cr, Mn, V, Mo)

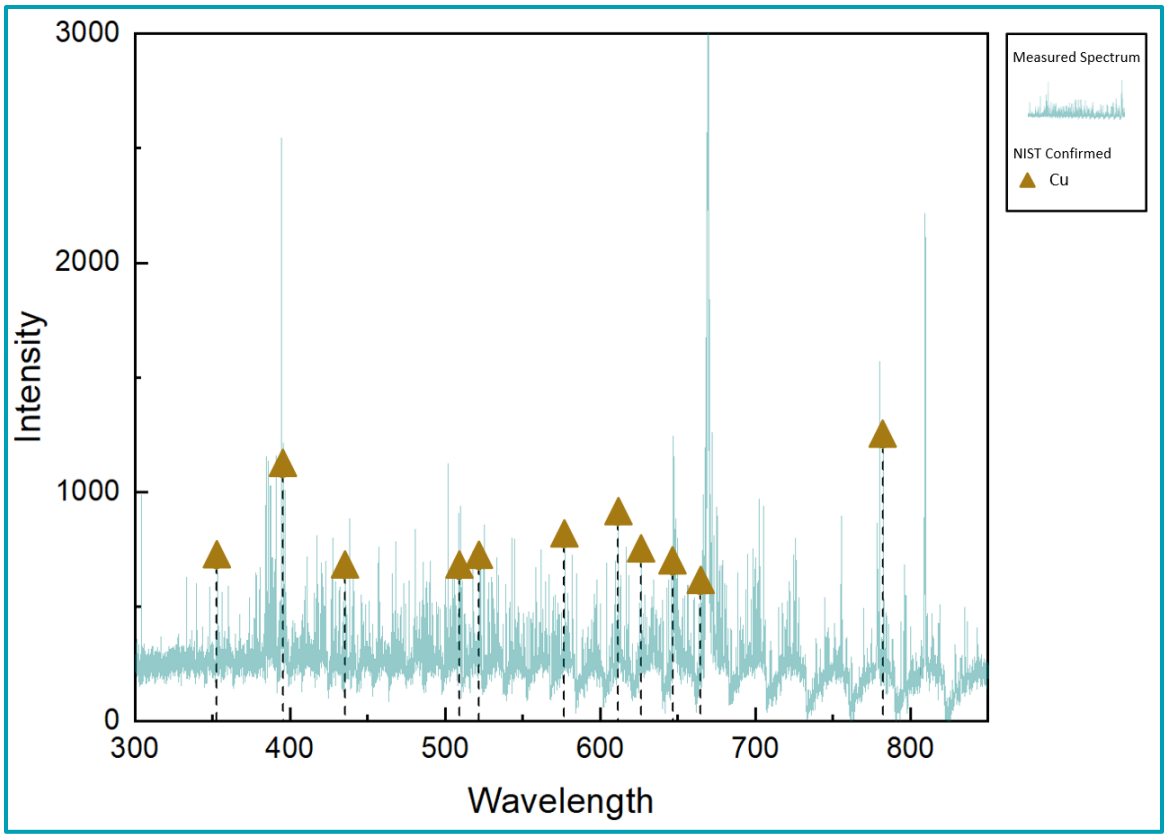

Figure 5.11 Chart showing sanitized data set of T5 with NIST confirmation where applicable

Table 5.13. T5 test results, observations and conclusions

Test ID	T5 flame with Eurocent (ablative)
Test type	Ablative
Capturing data successful	Yes
No. of frames captured	100 frames
Acceptable noise level	Partly, high noise on some frames
No. of spectral lines sufficient	Some frames – Low intensity
Usable frames	Yes
NIST confirmation of findings – rating	Yes – Excellent
Sufficient spectral lines per element	Yes
Dataset plotting worthy	Yes
Patterns of all elements convincing	Yes
Observations	
- The graph is coherent. - The overall count intensity is high. - The number of spectral lines is good.	

- All spectral lines are confirmed by the NIST Atomic Spectra Database.
- The spectral lines indicate detection of Cu traces with a probability bordering on certainty.
- The spectrum signature of the element is evidently visible.

Conclusions
- We can detect Cu in a flame using ablative LIBS.

5.7 Test 6 Exhaust Plume Emulation 4

The T6 test set up was identical to the set up in test T2. A little amount of metal scrap was dispensed in the flame while measuring. The data was analyzed for the Iron, Aluminum, Scandium, only.

Table 5.14 lists all elements that are present in the test under primary elements and other elements that are most likely present as well since they are in the surrounding air in possible wear debris from the burner under secondary elements. There is no graph since NIST confirmation fails. Table 5.15 provides an overview of the test quality, observations, and conclusions.

Table 5.14 T6 test overview

Test #	Test description	Primary elements	Secondary elements
T6	Flame with Scrap Metal	Fe, ??, ??, ??, H, C, O	N, Ar, Fe, Cu

Table 5.15. T6 test results, observations and conclusions

Test ID	T6 flame with scrap metal
Test type	Non-ablative
Capturing data successful	Yes
No. of frames captured	100 frames
Acceptable noise level	Partly
No. of spectral lines sufficient	Some frames
Usable frames	Yes
NIST confirmation of findings – rating	No – Need for more details
Sufficient spectral lines per element	Could not be determined
Dataset plotting worthy	No
Patterns of all elements convincing	No

Observations

- Analyzing is hard when you do not know where you are looking for.
- Could not find sufficient data different from T2 (flame only).
- The frames show many different patterns, might be many different elements.

Conclusions

- More in depth analytics is needed but is beyond the scope of this test.

6. Conclusions

A broad-scale of tests including non-ablative, ablative, non-luminous gaseous, and luminous gaseous LIBS tests have been executed, and these tests demonstrated that LIBS can be used to detect traces of elements under the testing conditions. Even the combination of non-ablative and luminous gaseous, which matches the rocket-engine exhaust plume most, confirmed that LIBS technology could support the wearing debris detection use case from a qualitative perspective. An additional number of tests using different scenarios for the non-ablative luminous gaseous exhaust plume environment are needed to determine the applicability from a quantitative perspective.

Looking at the datasets from a data quality perspective, then test 1a scored best, having a score of excellent for all quality parameters. The quality of the dataset is of great importance for unequivocal observations, pattern detection, and conclusion making. The existing experience with the original laser and the unfamiliarity with the ad hoc organized replacement laser seems to be a crucial factor, notwithstanding that the results with the replacement laser were unambiguous and suitable as well.

LIBS technology can provide a significant contribution to the safety of launch and space propulsion systems and therefore to unmanned and human space-travel and launch systems. LIBS technology can be applied in multiple phases of the system development life cycle, e.g., the design, testing, and maintenance phases but notably during operations as well. The small form-factor, limited weight, and acceptable power consumption need allow for incorporating LIBS as a smart sensor into the rocket engine and integration into the overall system health management ecosystem, providing useful data in real-time for fault detection, isolation, and recovery, for root cause analysis, trending, and predictive analytics.

The USB 3.0 UASP interface of the capturing camera allows for fast data transfers needed to accommodate the big data scenario of the intended use case. APIs in multiple programming languages and dynamic linking integration libraries, part of the SDKs made available by the equipment manufacturer, provide a command and control interface to operate the LIBS smart sensor in an orchestrated way by the system health management solution. The fact that the spectral lines from all elements are known and tagged, support supervised and hybrid machine learning scenarios. The standard operating procedure, as defined in this study, can be automated as well, ensuring that the smart sensor can function autonomously.

7. Outlook

LIBS has shown to be suitable for detecting traces of elements in luminous gaseous environments using a non-ablative methodology. The findings raise new questions that need to be examined like what will the postponed actual rocket-engine exhaust plume experiment reveal? What influence will the supersonic speeds in the nozzle have on the detectability? What happens when pressure conditions are changed? How do we get quantitative information from the measurements?

Other vital answers are needed on questions like, how can we optimize the detection of unexpected elements? What configuration of the LIBS system will generate the best results? What stack of big-data algorithms would work best to sanitize the data fast and provide unambiguous results? How much data is needed to predict remaining useful life?

Furthermore, what answers can LIBS technology not provide, can we combine LIBS with Raman? Can Raman spectroscopy provide insights on a molecular level in a high-speed luminous gaseous environment? Will Raman be useful to determine the effectiveness of the combustion process?

Optical sciences will play a major role in making space-travel safer. Not only for system health management applications, but also for monitoring the health of the crew, managing space habitats, or scan hazardous environments. Optical sciences can be used for spotting useful in-situ resources and scan the wider universe to collect data that will help us to find the answers we need and will provide better insights that empower better decision making, leading to better results, and making space-travel safer.

Boldly beyond!

8. Internship Reflection

The three-month internship at the DLR Institute of Space Propulsion in Lampoldshausen was a great experience I would not have missed. We visited DLR with ISU MSS19 for a Module 2 workshop, and I took the opportunity to network and to disseminate my "Make space-travel safer" mission and my idea to use Laser-Induced Breakdown Spectroscopy (LIBS) to monitor the rocket-engine exhaust plume for wear debris and possible other anomalies in an integrated system health management solution. These conversations led to my internship, where I could work on my idea and examine its feasibility.

Professional and personal benefits

Ranking the seven ISU disciplines by applicability to my internship resulted in the list below, starting with the most applicable.

1. Space Science
2. Space Engineering
3. Space Applications
4. 3I Space
5. Space Management and Business
6. Space Policy, Economics, Law
7. Human Performance in Space
8. Space Humanities

Space science is the area where my knowledge increased most, especially in subfields as atomic physics, molecular physics, atomic and molecular astrophysics, chemical physics, optics, photonics, laser physics, plasma physics, and astrodynamics.

Space engineering is a good second. I learned a lot on propulsion systems, rocket engines, cryogenics, combustion engines, control engineering, and materials science, to name a few. Moreover, I gained better insight into how large-scale laboratories and rocket-engine test benches are managed and operated.

There was a clear link with space applications as well. Applied technologies like optical spectroscopy are also used for Earth observation applications. LIBS is used on the Mars rover Curiosity and is a technology that can be used to scan asteroids to estimate their value mining.

For developing my 3I skills, DLR Lampoldshausen was a good place. The Institute of Space Propulsion is located in a quiet rural area but employs people from all over Europe and other parts of the world as well, creating an international-intercultural mix of people. After Germans the Italians are the largest group, followed by the French, who mainly work for CNES and the ArianeGroup. Other countries represented, that I know of, were

Australia, USA, Russia, Brazil, India, and the Netherlands. A couple of years ago there was a central student housing in Möckmühl, a medieval town ten minutes from DLR, but it was shut down, and students are spread across the region now. I was lucky that a DLR-ISU alumni event was organized during my stay, and I was able to meet fellow SSP18 participants and made some new contacts.

My feasibility study has a substantial space business component as well since it is the foundation for developing a new product to make space-traveling safer. I was also able to promote my idea to the commercial propulsion industry. During the internship it became evident that the space industry embraces the idea of using LIBS for monitoring the system health of propulsion systems, in multiple phases of the system development life cycle, including operations, making my internship from the Space Management and Business discipline standpoint a success as well.

Regarding the discipline Space Policy, Economics, and Law I learned a lot about the funding mechanism for research and development in Germany and how essential research institutions compete for funding and how they cooperate to realize critical large-scale scientific projects.

The hands-on experiments in the labs and rocket-engine test benches were very valuable as Confucius said +/- 2,500 ago:

> "Tell me, and I will forget.
> Show me, and I may remember.
> Involve me, and I will understand."

Information for prospective interns

The DLR Institute of Space Propulsion is a student-friendly workplace, the people are very supportive, there is no dressing code, and the company restaurant provides multiple menu choices each day for a student discount price. There are many projects with hands-on experiments, and before you know, you are conducting tests in one of the rocket-engine test benches or a laboratory.

The dangerous character of the rocket-engine tests and onsite cryogenic storage of propellants require strict security policies and it is vital to adhere to them. The policies do not influence the relaxed working atmosphere. German and English are widely spoken, though approximately 90% of the not project-related correspondence is in German. Safety training and other instructions are typically in German only. It is not necessary to speak German, but it makes life easier. A car makes life more comfortable as well since no public transportation is available to and from the institute.

If you come to Lampoldshausen, make time available for sightseeing this unique region with its lovely castles, fortresses, monasteries, medieval towns, and wineries that decorate the rolling landscape. Gliding is a popular recreational activity in this area where you can find many gliding airfields. Moreover, during the summer, many town festivals are organized, and Stuttgart is only one hour by car.

References

Alamgir, N., 2019. *Mars UI National Graphics*. [online image] Available at: <http://nawazalamgir.com/portfolio/mars> [Accessed 2 August 2019].

Andor Solis, n.d. *Solis 64 - Solutions for Imaging and Spectroscopy 64-bit acquisition software.* [pdf] Available at: <https://andor.oxinst.com/products/solis-software/solis-i> [Accessed 2 August 2019].

Andor, n.d. a. *Echelle Spectograph Overview | Flexible Spectroscopy Tool*. [online] Available at: <https://andor.oxinst.com/learning/view/article/echelle-spectrographs-a-flexible-tool-for-spectroscopy> [Accessed 2 August 2019].

Andor, n.d. b. *iStar sCMOS Ultrafast Platform for Nanosecond Time-resolved Imaging and Spectroscopy.* [online] Available at: <https://andor.oxinst.cn/assets/uploads/products/andor/documents/andor-istar-scmos-specifications.pdf> [Accessed 2 August 2019].

Andor, n.d.c. *How Does an Echelle Spectograph Work?*. [online] Available at: < https://andor.oxinst.com/learning/view/article/echelle-spectrographs> [Accessed 2 August 2019].

Baumgart, M., Glassl, A. and Kroupa, G., 2011. *Interferometric heat-load sensing of a high power solid laser medium*.[pdf] Available through: <https://www.ama-science.org/proceedings/getFile/ZmH2> [Accessed 12 August 2019].

Bernath, P., 2015. *Spectra of Atoms and Molecules.* 3rd ed. New York: Oxford University Press.

Biblarz, O. and Sutton, G. P., 2016. *Rocket Propulsion Element*s. New York: John Wiley & Sons, Incorporated.

Bob, 2018. *2201 Spectroscopy: Quantization of energies*. [online] Available at: <http://www.ahachemistry.com/2201-spectroscopy-quantization-of-energies.html> [Accessed 2 August 2019].

Börner, M. and Kroupa, G., 2018. A miniaturized high energy laser for ignition of rocket engines. *International Conference on Space Optics - ICSO 2018.* Chania, Greece, 9-12 October 2018.

Bruckner, G., Kroupa, G. and Rackemann, N., 2017. Laser Ignition for Aerospace Applications using the Rugged Miniaturized HiPoLas® Nd-YAG Laser System. *The Optical Publishing, Laser Ignition Conference 2017*. Bucharest, Romania, 20-23 June 2017.

Crystal Techno, n.d. *Sapphire Spherical Plano-Convex Lenses*. [online] Available at: <http://www.crystaltechno.com/Al2O3_pl-cvx_en.htm> [Accessed 15 August 2019].

Deekena, J., dos Santos Hahna, R., Traudta, T,. Wagnera, B. and Waxenegger-Wilfinga, G., 2017. An Overview on the Turbopump Roadmap for the LUMEN Demonstrator Engine and on the new Turbine Test Facility. DLR Institute of Space Propulsion, *68th International Astronautical Congress (IAC).* Australia, Adelaide, 25-29 September 2017. Paris: IAF.

DLR Institute of Space Propulsion, 2007. *Institut Für Raumfahrtantriebe Europäischer Forschungs- Und Technologie-Prüfstand P8* (in German). [online] Available at: <https://www.dlr.de/Portaldata/55/Resources/dokumente/P8D-Vorlage.pdf> [Accessed 2 August 2019].

DLR Institute of Space Propulsion, 2016. *Test Facility M11*. [pdf] Available at: <https://www.dlr.de/ra/Portaldata/55/Resources/dokumente/2016.03.21_Handout_M11_final.pdf> [Accessed 2 August 2019].

DLR Institute of Space Propulsion, 2017. *Institute of Space Propulsion Lampoldshausen*. [pdf] German Aerospace Center Institute of Space Propulsion. Available at: <https://www.dlr.de/ra/Portaldata/55/Resources/dokumente/2017/Institute_of_Space_Propulsion_-_Status_Report_2017.pdf> [Accessed 2 August 2019].

DLR Institute of Space Propulsion, 2018. *DLR Site Lampoldshausen an Overview*. [pdf] German Aerospace Center Institute of Space Propulsion. Available at: <https://www.dlr.de/dlr/de/Portaldata/1/Resources/bilder/portal/lampoldshausen/lampoldshausen_2018/DLR_Standortflyer_Lampoldshausen_GB_web.pdf> [Accessed 2 August 2019].

DLR, 2019. *DLR at a Glance*. [online] Available at: <https://www.dlr.de/dlr/en/desktopdefault.aspx/tabid-10443/637_read-251/#/gallery/8570> [Accessed 2 August 2019].

DLR, n.d. a. *Space Propulsion Departments*. [online] Available at: <https://www.dlr.de/ra/en/desktopdefault.aspx/tabid-4041/> [Accessed 2 August 2019].

DLR, n.d. b. *Test Facility Department*. [online] Available at: <https://www.dlr.de/ra/en/desktopdefault.aspx/tabid-8483/14618_read-36493> [Accessed 2 August 2019].

Embry-Riddle, 2019. *Linear Momentum and Collisions*. [online] Available at: < http://physicsx.pr.erau.edu/Courses/CoursesSummerA2019/PS113/Lectures%20Open%20Stax/Chapter%208%20CollegePhysics-OP.pdf> [Accessed 2 August 2019].

ESA, 2016. *Launchers Access to Space – Ariane 5 ECA*. [online] Available at: < http://m.esa.int/Our_Activities/Space_Transportation/Launch_vehicles/Ariane_5_ECA2 > [Accessed 2 August 2019].

Figueroa, F., Morris, J., Kapadia, R., Schmalzel, J., Smith, H., Turowski, M., Venkatesh, M. and Walker, M., 2009. *Integrated System Health Management: Foundational Concepts, Approach, and Implementation*. NASA Integrated System Health Management. AIAA Infotech at Aerospace Conference and Exhibit and AIAA Unmanned...Unlimited Conference. Seattle, Washington, 6-9 April 2009. Atlanta: AIAA Meeting Paper.

Garg, S., Maul, W.A. and Melcher, K.J., 2007. Propulsion Health Management System Development for Affordable and Reliable Operation of Space Exploration Systems. In:AIAA (American Institute of Aeronautics and Astronautics), *AIAA SPACE 2007 Conference and Exposition.* Long Beach, California, 18-20 September 2007. Cleveland, Ohio.

Gurnett, D. and Bhattacharjee, A., 2005. *Introduction to plasma physics: with space and laboratory applications*. Cambridge: Cambridge University Press.

Google maps, 2019. *Satellite photo of the DLR Institute for Space Propulsion – Hardthausen am Kocker,* 49°16'57.0"N 9°22'25.8"E. [online] Available through: <https://goo.gl/maps/RPjc3FThuLFGQhbw6> [Accessed 12 August 2019].

Hänsch, T. and Träger, F., 2007. *Spring Handbook Lasers and Optics*. 2nd ed. New York: Springer.

Helmholtz, 2019a. *The Helmholtz Association*. [online] Available at: <https://www.helmholtz.de/en/about_us/the_association/> [Accessed 2 August 2019].

Helmholtz, 2019b. *Facts and Figures*. [online] Available at: <https://www.helmholtz.de/en/about_us/the_association/facts_and_figures/> [Accessed 2 August 2019].

Iumtek, n.d. *Definition of LIBS*. [online] Available at: <https://iumtek.com/en/libs-technology/> [Accessed 2 August 2019].

Johnson, B., S., Gormley, T., Kessler, S., Mott, C., Patterson-Hine, A., Reichard, K. and Scandura, P., 2011. *System Health Management: with Aerospace Applications*. New York: Wiley, Hoboken.

Kenyon, I., 2011. *The Light Fantastic: A Modern Introduction to Classical and Quantum Optics.* 2nd ed. New York: Oxford University Press.

Lab Unlimited, n.d. *Camping Gaz Gas Cartridges C 206 Cap. 190g 203 531*. [online] Available at: <https://www.labunlimited.com/s/ALL/4AJ-9018520/Camping-Gaz-Gas-Cartridges-C-206-Cap.-190g-203-531> [Accessed 2 August 2019].

LibreTexts, 2019. *Summary of possible Phase Transitions*. [image online] Available at: <https://phys.libretexts.org/Courses/University_of_California_Davis/UCD%3A_Physics_7A/1%3A_Applying_Models_to_Thermal_Phenomena/1.3%3A_Three_Phase_Model_of_Matter> [Accessed 2 August 2019].

More, N., 2017. *Optical Characterization of Laser Induced Helium Plasmas*. [pdf] Available at: <https://www.researchgate.net/publication/322404442_Optical_Characterization_of_Laser_Induced_Helium_Plasmas> [Accessed 2 August 2019].

Musazzi, S. and Perini, U., 2014. *Laser-Induced Breakdown Spectroscopy – Theory and Applications*. Springer: New York.

NASA, 2001. *NASA Chapter 7: Plasma.* [online] Available at: <https://www-spof.gsfc.nasa.gov/Education/wplasma.html> [Accessed 2 August 2019].

NIST, 2018. *Atomic Spectra Database - NIST Standard Reference Database 78*. [online] Available at: < https://www.nist.gov/pml/atomic-spectra-database> [Accessed 2 August 2019].

OriginLab, n.d. *Origin and OriginPro Introduction*. [online] Available at: <https://www.originlab.com/index.aspx?go=Products/Origin> [Accessed 2 August 2019].

Peek, H., 2010 *The emergence of the compact disc.* [e-journal] 48(1), pp. 10-17. Abstract only. Available through: IEEE Communications Magazine website < https://ieeexplore.ieee.org/document/5394021> [Accessed 2 August 2019].
Plasma Universe, n.d. *Plasma*. [online] Available at: <https://www.plasma-universe.com/plasma> [Accessed 2 August 2019].

Quantel Laser, 2013. *Q-smart 450/850 User Manual*. [pdf] Lannion: Quantel.

Richmond., M., 2012. *Physics 301, "University Astronomy", Spring 2011*. [online] Available at: <http://spiff.rit.edu/classes/phys301/phys301.html > [Accessed 2 August 2019].

Stützer, R., Börner, M. and Oschwald, M., 2018. *Optical Characterization of the Laser-Induced Ignition Spark in a Cryogenic Rocket Combustor*. [e-journal] 17(4), pp. 337-347. Available through: ResearchGate GmbH. Website < https://www.researchgate.net/publication/330547703_Optical_Characterization_of_the_Laser-Induced_Ignition_Spark_in_a_Cryogenic_Rocket_Combustor> [Accessed 2 August 2019].
Swinerd, S., 2008. *How Spacecraft Fly: Spaceflight Without Formulae*. Springer: New York. pp.103-104.

ThorLabs, 2000. *LB4265 - f = 150.0 mm, Ø1" UV Fused Silica Bi-Convex Lens, Uncoated*. [online] Available at: <https://www.thorlabs.com/thorproduct.cfm?partnumber=LB4265 > [Accessed 2 August 2019].

ThorLabs, 2014. *DMLP950 - Ø1" Longpass Dichroic Mirror, 950 nm Cut-On*. [online] Available at: <https://www.thorlabs.com/thorproduct.cfm?partnumber=DMLP950> [Accessed 2 August 2019].

UC Davis, 2019. *Summary of possible Phase Transitions*. [image online] Available at: <https://phys.libretexts.org/Courses/University_of_California_Davis/UCD%3A_Physics_7A/1%3A_Applying_Models_to_Thermal_Phenomena/1.3%3A_Three_Phase_Model_of_Matter> [Accessed 2 August 2019].

University of Windsor, n.d. *What is LIBS?*. [online] Available at: <http://www1.uwindsor.ca/people/rehse/15/what-is-libs> [Accessed 2 August 2019].

van Noetsele, L., 2018. *Scientific Florida inc. at NASAiTech Ignite the Night at the 34th Space Symposium*. [speech] (Personal communication, 17 April 2018).

Xu, T., Zhang, Y. and Zhao, Z., 2016 *Characterization of local thermodynamic equilibrium in a laser-induced aluminum alloy plasma.* [e-journal] 55(10), pp. 2741-2747. Available through: OSA Publishing Applied Optics Website <https://www.osapublishing.org/ao/viewmedia.cfm?uri=ao-55-10-2741&seq=0> [Accessed 2 August 2019].